Pergamon

Bioorganic & Medicinal Chemistry 6 (1998) 85–102

BIOORGANIC & MEDICINAL CHEMISTRY

Synthesis of key sandramycin analogs: systematic examination of the intercalation chromophore

Dale L. Boger*, Jyun-Hung Chen, Kurt W. Saionz, Qing Jin

Department of Chemistry and The Skaggs Institute of Chemical Biology, The Scripps Research Institute, 10550 North Torrey Pines Road, La Jolla, California 92037, USA

Received 28 August 1997

Abstract

The preparation and examination of **2–22** constituting a systematic study of the chromophore of sandramycin (**1**) are detailed. Fluorescence quenching studies were used to establish binding constants for **1–24** within calf thymus DNA, within a single high affinity bis-intercalation binding site 5′-d(GCATGC)$_2$, and to establish the preference for sandramycin binding to 5′-d(GCXXGC)$_2$ where XX = AT, TA, GC, and CG. From the latter studies, sandramycin was found to exhibit a preference that follows the order: 5′-d(GCATGC)$_2$ > 5′- d(GCGCGC)$_2$, $\Delta\Delta G^\circ = 0.3$ kcal/mol > 5′-d(GCTAGC)$_2$, 5′-d(GCCGGC)$_2$, $\Delta\Delta G^\circ = 0.6$ kcal/mol although it binds with high affinity to all four deoxyoligonucleotides. The two highest affinity sequences constitute repeating 5′-PuPy motifs with each intercalation event occurring at a 5′-PyPu step. The most effective sequence constitutes the less stable duplex, contains the sterically most accessible minor groove central to the bis-intercalation site, and the ability to accept two gly-NH/T C2 carbonyl H-bonds identified in prior NMR studies. Similarly, the contribution of the individual structural features of the chromophore were assessed with the high affinity duplex sequence 5′-d(GCATGC)$_2$. To a first approximation, the cytotoxic properties were found to parallel trends established in the DNA binding affinities. The exception to this generalization was **4** which lacks the sandramycin chromophore phenol. Although typically 4–10× less potent than sandramycin against leukemia cell lines, it proved to be 1–10,000× more potent against melanomas, carcinomas, and adenocarcinomas exhibiting IC_{50} values of 1 pM–10 nM placing it among the most potent agents identified to date. Additionally, the first disclosure of the HIV-1 reverse transcriptase inhibitory activity of sandramycin (**1**) as well as that of its key analogs are described and define the chromophore structural features required for their exceptional potency. Two analogs, **18** and **3**, roughly maintain the HIV-1 reverse transcriptase inhibitory potency of **1** but exhibit substantially diminished cytotoxic activity (10^2–10^3×).

1. Introduction

Sandramycin (**1**), a potent antitumor antibiotic [1] structurally characterized through spectroscopic and chemical degradation studies [2], constitutes one of the newest members of a growing class of cyclic decadepsipeptides including luzopeptins A–C and E_2 [3], quinaldopeptin [4] and quinoxapeptins A and B [5] which possess potent antitumor, antiviral, and antimicrobial activity (Fig. 1) [3–5]. Characteristic of this class of agents, sandramycin possesses a two-fold axis of symmetry and two heteroaromatic chromophores that results in sequence-selective DNA bis-intercalation spanning two base-pairs preferentially at 5′-AT sites [6–9]. In this respect, the agents are functionally related to the quinoxaline antitumor antibiotics [10] including echinomycin and triostin A which also bind to DNA by bis-intercalation but with a substantially different sequence selectivity (5′-CG versus 5′-AT) [11,12].

The cytotoxic activity of luzopeptin A and sandramycin has been shown to be 100–300× greater than echinomycin and smoothly declines in the series with luzopeptin A > B > C. A reverse order of antiviral activity was observed with luzopeptin C > B > A in inhibiting human immunodeficiency virus (HIV) replication in

*Corresponding author.

0968-0896/98/$19.00
PII: S0968-0896(97)10014-1

vitro. Notably, this is observed at noncytotoxic concentrations for luzopeptin C through inhibition of HIV reverse transcriptase [13]. The recent disclosure of the quinoxapeptins as potent inhibitors of HIV-1 and HIV-2 reverse transcriptase that are equally active against two resistant single mutants and a double mutant of HIV-1 reverse transcriptase has increased the interest in this class of agents especially since they were found not to inhibit human DNA polymerase α, β, γ, and δ at comparable concentrations [5].

We recently reported a convergent total synthesis of sandramycin in which the heteroaromatic chromophores were introduced in the final stages [6]. This not only provided sufficient quantities of the natural product to define its DNA binding properties, but also the key partial structures lacking one or both of the pendant chromophores. This has now been extended to the preparation of **2–22** differing only in the structure of the pendant chromophore (Fig. 2). Using this approach, incremental changes in the chromophore were used to assess the role of each of its structural components.

DNase I footprinting experiments have demonstrated that sandramycin, like the luzopeptins [7], shows a slight preference for regions of DNA containing alternating A and T residues with a perceptible preference for 5′-AT dinucleotide sequences most often preceded by a 5′-C, (i.e. 5′-CAT) [6]. As with the luzopeptins [9], the binding mode was confirmed by ^{1}H NMR studies of a C_2-symmetric 1:1 complex of sandramycin with 5′-d(GCATGC)$_2$ in which the agent was found to bind by bis-intercalation about the central 5′-AT base-pairs [6]. DNA binding affinity established by fluorescence quenching of the agent with calf thymus DNA revealed that sandramycin ($3.4\times10^7\,M^{-1}$) exhibited a slightly higher apparent binding constant than luzopeptin A ($1.2\times10^7\,M^{-1}$) [6]. A larger base-pair:agent ratio was also found for sandramycin, 1:6.7 versus 1:4.5, implying an increased selectivity. Although these studies demonstrated effective bis-intercalation at 5′-AT, they did not exclude the possibility of binding at other sites. This possibility was supported by footprinting experiments

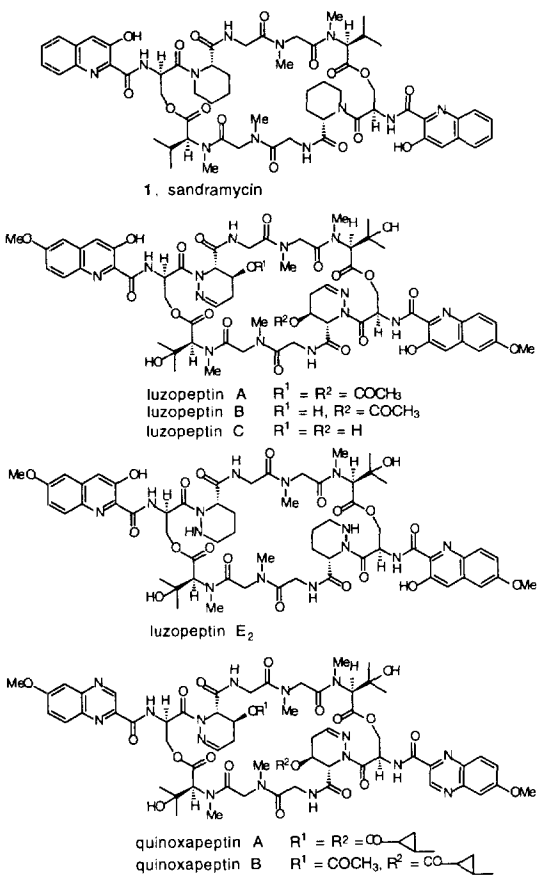

Fig. 1.

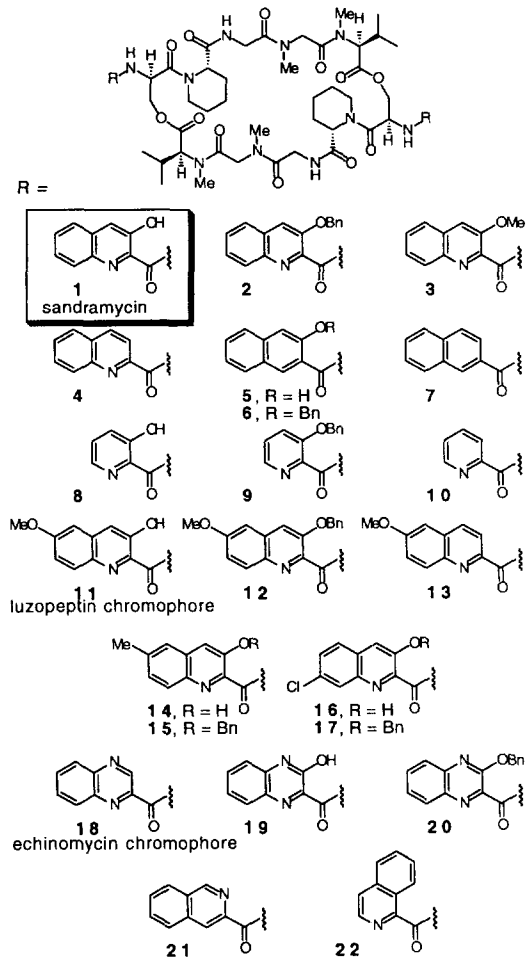

Fig. 2.

which showed that at low agent concentrations, 5′-AT and especially 5′-CAT sites were protected but at moderate agent concentrations, the DNA was almost evenly protected from digestion [6]. In order to probe this binding selectivity, herein we provide details of the comparative binding of sandramycin with 5′-d(GCXXGC)$_2$ where XX = AT, TA, GC, and CG.

In our prior studies, the binding affinity of **23** and **24** with calf thymus DNA was established to be 2.4 $\times 10^4\,M^{-1}$ and $5.7\times 10^6\,M^{-1}$, respectively (Fig. 3). Thus, the incremental addition of the chromophores to **23** ($\Delta G^\circ = -6.0$ kcal/mol) increase the binding by 3.2 and 1.0 kcal/mol, respectively. This is consistent with the representation of sandramycin and the luzopeptins as minor groove binding cyclic decadepsipeptides incrementally stabilized by mono- and bis-intercalation. To further define the role of the chromophores, the binding affinity of **2–22** with both calf thymus DNA and 5′-d(GCATGC)$_2$ are also described. In these studies, the correlation of structural changes in the chromophore with the resulting changes in the binding affinity not only permitted the determination of the structural features contributing to the high affinity bis-intercalation binding, but their absolute magnitude as well.

2. Preparation of 3–22

The synthesis of the agents including those that contain the luzopeptin or echinomycin chromophores required *N*-BOC deprotection of **23**[6] ($[\alpha]_D^{23}$ −53 (*c* 0.15, $CHCl_3$), 3 M HCl–EtOAc, 25°C, 30 min), coupling of the resulting bis amine **25** with the appropriate carboxylic acids (4 equiv. of EDCI, 6.0 equiv. of HOBt, 10 equiv. of $NaHCO_3$, DMF, 25°C, 48–72 h, 76–94%) and, when required, final deprotection of the bis-*O*-benzyl derivatives **6**, **9**, **12**, **15**, **17** or **20** (H_2, 10% Pd–C, EtOAc, 25°C, 14–24 h, 78–94%). This is illustrated in Scheme 1

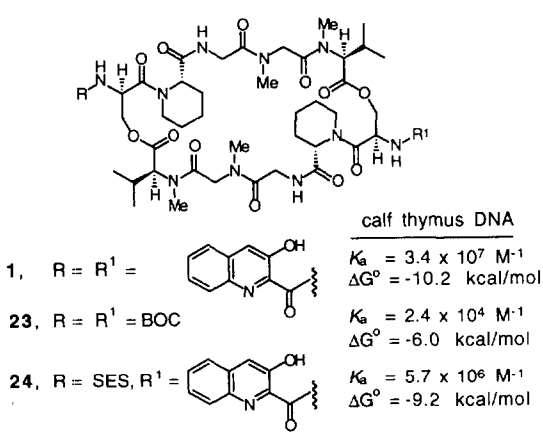

Fig. 3.

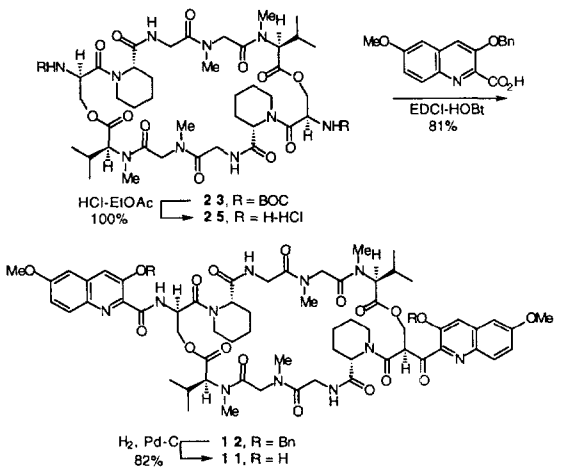

Scheme 1.

with the preparation of **11** and **12** which constitutes the incorporation of the luzopeptin chromophore into the sandramycin structure.

The required four carboxylic acids for the introduction of the chromophores of **1–2**, **11–12**, **14–15**, and **16–17** were derived through use of a modified Friedlander condensation [14] employing the readily accessible *O*-methyloxime (Scheme 2) as recently detailed [15].

The aryl 3-benzyloxy-2-carboxylic acids required for introduction of the chromophores for **5–6**, **8–9**, and **19–20** were prepared by perbenzylation of the corresponding 3-hydroxy-2-carboxylic acids (3 equiv. BnBr, K_2CO_3,

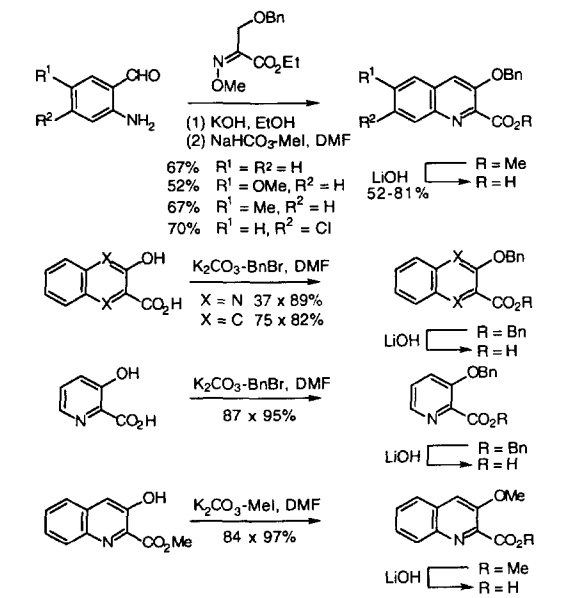

Scheme 2.

DMF, 25°C, 4 h) followed by hydrolysis of the resulting benzyl ester (LiOH, THF–CH_3OH–H_2O, 25°C). Similarly, the chromophore for **3** was prepared by *O*-methylation of methyl 3-hydroxyquinoline-2-carboxylate [15] (CH_3I, K_2CO_3, DMF, 25°C, 84%) followed by methyl ester hydrolysis. 6-Methoxyquinoline-2-carboxylic acid was obtained by hydrolysis of 2-cyano-6-methoxyquinoline [16] (25% aqueous NaOH, CH_3OH, 80%, 4 h, 77%). The remainder of the carboyxlic acids used for the chromophore introduction were commercially available.

2.1 Conformational properties of **1** *and the related cyclic decadepsipeptides*

The single crystal X-ray structure determination of **23** [6] revealed a backbone conformation nearly identical to that of luzopeptin A [3c]. The most significant perturbation of the two structures was the twisted orientation of the linking esters. The relative placement of the ring nitrogens and the backbone conformation of the pentapeptides excluding the ester atoms are even more similar in the two structures. The overall shape of the agent is rectangular with a twofold axis of symmetry. The long sides of the rectangle consist of antiparallel and twisted β-extended chains capped on either end by the two decadepsipeptide ester linkages. Each of the amides including the three tertiary amides adopt a trans or extended stereochemistry and the two decadepsipeptide esters adopt the preferred syn conformation. The two symmetrical secondary amide NHs of glycine are engaged in tight transannular H-bonds (2.08 Å, gly-NH–O=C-gly) to the glycine carbonyl oxygen across the ring and cap two reverse peptide turns induced in part by the incorporation of unnatural D-serine at one corner of each turn. The pipecolic acid residue adopts a classical chair conformation with the α-carboxylate adopting an axial position and skewed by approximately 48° from the optimal anti relationship of the carbonyl to the Cα-H. In this conformation the D-ser-NH/D-ser-NH distance is 15.1 Å. The comparable luzopeptin A D-ser-NH/D-ser-NH distance is 14.8 Å and the distance between the centers of the two chromophores in this X-ray is 17.4–19.9 Å. The 1-D ^{1}H NMR of **2–22** indicate that they adopt a single, rigid solution conformation comparable to that observed with sandramycin and **23** which have been examined in detail [6]. In all solvents except DMSO-d_6, the agents adopted a single, rigid solution conformation comparable to that observed in the X-ray. This conformation is inherent in the cyclic depsidecapeptide and independent of the pendant chromophore.

As discussed in detail [6,9], the bis-intercalation spans two base-pairs and requires the adoption of a conformation in which the two chromophores are separated by 10.1–10.2 Å. However, the X-ray conformation and the related solution phase conformation of **1–22** adopt a more extended conformation in which the interchromophore distance is 17–19.5 Å. Thus, the agents must adopt an altered conformation upon bis-intercalation DNA binding that is substantially different than its preferred native X-ray or solution conformation. Both the pip-gly secondary amides and the tertiary gly-sar amides adopt cis versus trans amide stereochemistries in order to accommodate this shorter distance and the bound conformations of the agent maintains its twofold axis of symmetry. The gly NHs are reoriented to form intermolecular H-bonds with the thymine C2 carbonyls and nicely explain the preference for the 5′-AT sequence. Complementary intermolecular hydrophobic contacts extend over much of the interacting surface. These observations have suggested that the relatively low contribution to the binding affinity attributable to the second intercalation is due to an accompanying destabilizing conformational change in the cyclic decapeptide that offsets much of the gains derived from a second intercalation.

3. DNA binding affinity and selectivity

Apparent absolute DNA binding constants for **1–22** and related agents including luzopeptin A were obtained by measurement of the fluorescence quenching upon titration addition of calf thymus DNA or the deoxyoligonucleotides 5′-d(GCXXGC)$_2$ where XX = AT, TA, GC, and CG [6,8]. For each agent, the characteristic fluorescence excitation and emission spectra were recorded in 10 mM Tris-HCl, 75 mM NaCl (pH 7.4) buffer (Table 1). For the DNA binding assays

Table 1
Fluorescent excitation wavelengths, emission wavelenghts and percent quenching of analog fluorescence

Analog	Excitation (nm)	Emission (nm)	% Quenching[a]
1	364	532	76
	—	—	89[b]
	—	—	80[c]
	—	—	91[d]
3	339	418	89
4	286	410	79
8	311	411	60
11	341	532	75
13	335	422	81
14	358	534	69
16	368	536	83
17	345	412	52
21	324	420	92
22	325	420	84
24	360	511	60

[a]With 5′-d(GCATGC)$_2$.
[b]5′-d(GCGCGC)$_2$.
[c]5′-d(GCTAGC)$_2$.
[d]5′-d(GCCGGC)$_2$.

which quantitate the fluorescence quenching, excitation outside the absorbance range of DNA was employed and the most intense fluorescence emission at a longer wavelength monitored. For assay of the DNA-induced fluorescence quenching of the agents, a 2 ml buffer solution of Tris-HCl (pH 7.4) and 75 mM NaCl was employed. For titration, small aliquots of DNA were added to solutions of the agents in Tris-HCl buffer (pH 7.4).

The addition of DNA caused a marked quenching effect on the fluorescence of the agents. The DNA quenching of fluorescence ranged from 52–92% as summarized in Table 1. The analogs **5**, **7**, **18**, and **19** were not sufficiently soluble to examine in this assay. Due to the inner filter effect, choosing the excitation wavelength at a UV absorbance peak maximum may lead to non-linear Beer's law plots of intensity versus concentration affecting the results of the fluorescence quenching studies [17]. However, plots of fluorescence versus intensity proved to be linear throughout the concentration ranges in our study. To minimize fluorescence decrease due to dissolution or photobleaching, the solutions were stirred in 4 ml quartz cuvettes shielded from light in a darkened room with the minimum exposure to the excitation beam necessary to obtain a reading. Despite these precautions, the fluorescence for a number of the analog solutions decreased for several analogs (**11**, **14**, **17**, **21**, and **22**) and the quality of the binding constants for these should be viewed with caution. The fluorescence decreases were not effected by taking multiple readings indicating that the observations are not due to photobleaching. This effect was less significant in the quartz versus plastic cuvettes and could be minimized by increasing the concentration of DMSO suggesting the effects may be due to aggregate formation. The titrations were carried out with 15 min time intervals between DNA additions to allow binding equilibration. Notable differences have not been detected with different time intervals (10–30 min) indicating that tight binding equilibration is rapid. The results of the study are summarized in Table 2. The titration fluorescence quenching was analysed by Scatchard analysis [18] as previously detailed [6,8] with the following equation: $r_b/c = K_b n - K_b r_b$ where r_b is the number of agent molecules bound per DNA base-pair, c is the free drug concentration, K_b is the apparent association constant, and n is the number of agent binding sites per base-pair. From a plot of r_b/c versus r_b as shown in Fig. 4 for **4**, association constants (K_b) for **1–22** and luzopeptin A were derived from the slope and the binding site sizes determined from the x-intercept values (n) for the number of agent binding sites per base-pair. The results are summarized in Table 2.

Typical of such studies [19], the Scatchard plots exhibited a downward convex curvature that reduced to straight lines at the extremes indicating high and low affinity binding. A pronounced downward curvature in an infinite lattice such as calf thymus DNA is recognized to arise in part from neighbor exclusion where the binding of an agent excludes the subsequent binding at nearby sites. This exclusion manifests itself in the plot by a reduction in the apparent binding constant as the DNA lattice approaches saturation and the probability of finding a free site is diminished. In the calf thymus DNA studies, the binding also entails multiple classes of independent binding sites or modes. For simplicity, a linear fit of the high affinity binding sites was used to determine the binding constant attributable to bis-intercalation [20]. For the deoxyoligonucleotides, the curvature can be more simply attributed to multiple classes of independent binding sites or binding modes [21]. There are a number of mathematical methods to deconvolute the curved plot into such individual binding

Table 2
Calf thymus DNA and 5′-d(GCATGC)$_2$ binding

Analog	Calf thymus DNA		5′-(GCATGC)$_2$			
	K_b (M^{-1})[a]	$\Delta G°$ (kcal/mol)	K_b (M^{-1})[a]	$\Delta G°$ (kcal/mol)	K_b (M^{-1})[b]	$\Delta G°$ (kcal/mol)
1	1.6×10^7	−9.8	6.4×10^7	−10.6	2.3×10^8	−11.4
3	3.7×10^6	−9.0	1.3×10^7	−9.7	1.7×10^7	−9.9
4	3.2×10^6	−8.9	1.4×10^7	−9.7	2.5×10^7	−10.1
8	8.3×10^5	−8.1	1.3×10^6	−8.3	3.0×10^6	−8.8
11	8.3×10^6	−9.4[c]	2.6×10^7	−10.1	5.1×10^7	−10.5
13	4.8×10^6	−9.3	6.4×10^6	−9.3	1.6×10^7	−9.8
14	5.8×10^6	−9.2[c]	2.5×10^7	−10.1	2.9×10^7	−10.2
16	7.6×10^6	−9.4	3.6×10^7	−10.3	7.3×10^7	−10.7
17	1.3×10^5	−7.0	3.5×10^5	−7.6	nd	—
21	nd	—	3.5×10^6	−8.9	4.3×10^5	−7.7[c]
22	3.2×10^6	−8.9[c]	3.4×10^6	−8.9	8.0×10^6	−9.4

[a]Linear fit of high affinity sites.
[b]Non-linear fit of all sites.
[c]Background fluorescence decrease subtracted out, see text.

events. In the deoxyoligonucleotide studies, a non-linear fit described by Feldman was also used to deconvolute the curves [21]. The model assumes one ligand with two binding types or sites. Since the number of binding sites is limited, we have interpreted this to indicate a high affinity bis-intercalation and a lower affinity binding potentially involving mono-intercalation. The equation fits r_b to r_b/c according to the following equation:

$$\frac{r_b}{c} = \frac{1}{2}\left(K_1(n_1 - r_b) + K_2(n_2 - r_b) + \sqrt{(K_1(n_1 - r_b) - K_2(n_2 - r_b))^2 + 4K_1K_2n_1n_2} \right)$$

where K_1 and K_2 represent the association constants for high and low affinity binding and n_1 and n_2 represent the number of bound agents per duplex for the separate binding events. The formula was fit using the JMP [22] statistical fitting program using an initial approximation of the two n values and fitting for K_1 and K_2. Regardless of the interpretation, the results obtained taking into account the lower affinity binding with the second method provides a slightly higher binding constant for the high affinity binding event but, in general, did not alter the overall qualitative or relative quantitative trends in binding.

The studies with calf thymus DNA and 5′-d(GC-ATGC)$_2$ provided comparable results. Both the relative trends in binding affinity and the quantitative differences

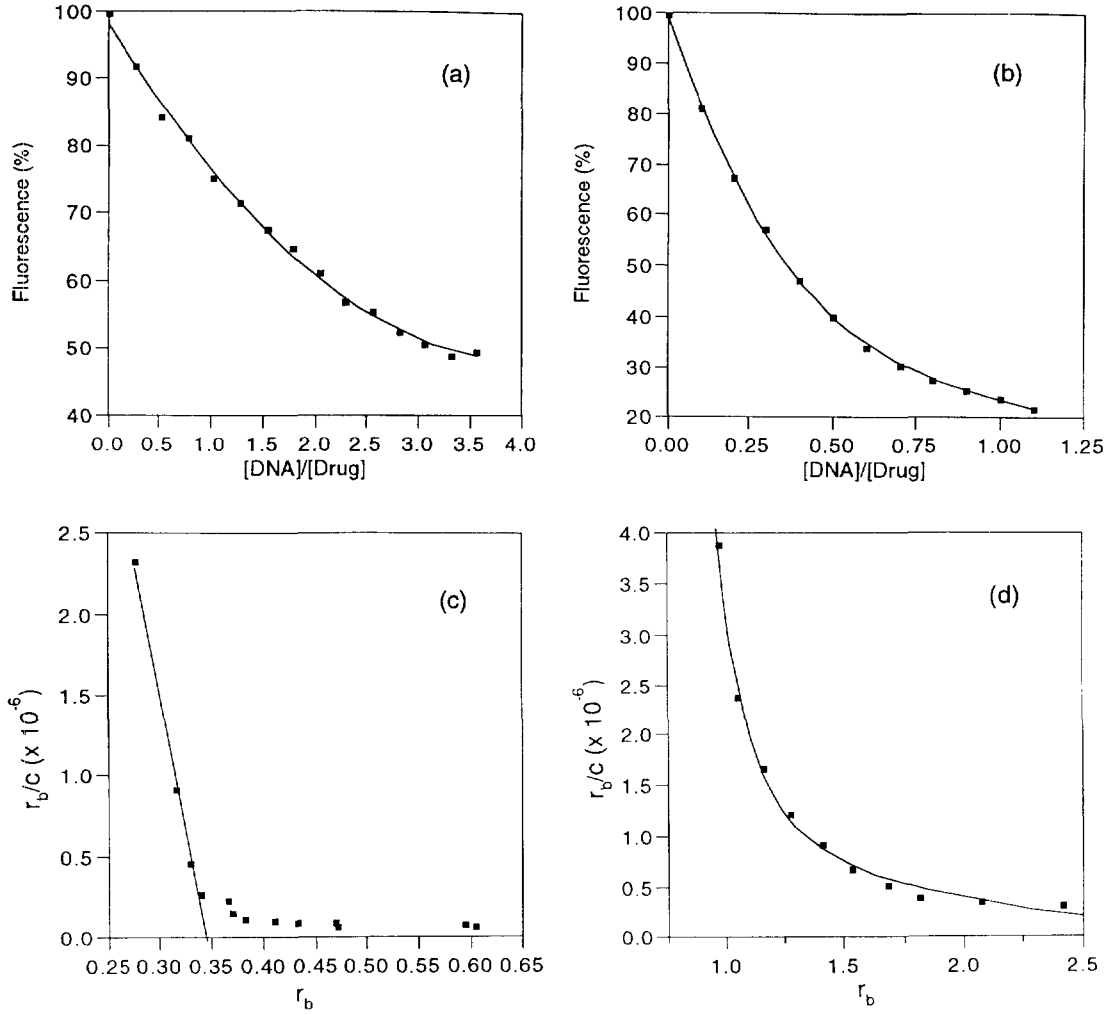

Fig. 4. Fluorescence quenching of agent **4** (excitation at 286 nm and emission at 410 nm in 10 mM Tris-HCl (pH 7.4) and 75 mM NaCl buffer solution) with (a) increasing calf thymus DNA concentration and (b) increasing 5′-d(GCATGC)$_2$ concentrations. Scatchard plots of fluorescent quenching of agent **4** with (c) calf thymus DNA (linear fit of high affinity sites) and (d) 5′-d(GCATGC)$_2$ (non-linear fit).

were comparable regardless of the DNA employed although the deoxyoligonucleotide typically provided higher binding constants. We attribute this to the difference in measuring the absolute binding constant at a single high affinity site within 5′-d(GCATGC)$_2$ versus the apparent absolute binding constant for the composite of sites within calf thymus DNA. Several important trends emerged from these studies, (Fig. 5). First, either *O*-methylation of the chromophore phenol or its removal altogether resulted in a comparable reduction of the binding affinity. This typically proved to be worth 1.5–0.8 kcal/mol (**1** versus **3** and **4**). This suggests that each hydroxyl group contributes approximately 0.5 kcal/mol toward the binding affinity of sandramycin. Similar trends were observed in comparing **11** and **13**. In contrast to this modest effect, *O*-benzylation of the chromophore phenol had a much larger effect reducing the binding affinity by 2.4–2.7 kcal/mol (**16** versus **17**). Thus, significant perturbations including the complete removal of the phenol may be well tolerated while more substantial changes including the substitution with large groups (i.e. *O*-benzylation) substantially reduces the binding affinity providing agents that are only comparable to **23** which lacks both chromophores altogether. Secondly, the luzopeptin chromophore proved slightly less effective illustrating that the C6 methoxy group is not contributing significantly or productively to the DNA binding affinity (**1** versus **11**). Similar observations were made in the comparisons of **4** with **13**. Likewise, the introduction of a C6 methyl group (**14**) or C7 chlorine substituent (**16**) did not have a substantial effect on the DNA binding affinity although **16** typically was nearly indistinguishable from **1** while **14** was consistently slightly less effective. Thus, significant perturbations at the C6 and C7 positions are tolerated although none were found to productively contribute to DNA binding affinity. The reduction of the chromophore to the 3-hydroxypyridine-2-carboxylate with removal of the fused benzene ring with **8** resulted in a large drop in DNA binding affinity costing 1.7 kcal/mol in calf thymus DNA and 2.3–2.6 kcal/mol with 5′-d(GCATGC)$_2$. Finally, the behavior of **21** and **22** relative to **1** and **4** proved interesting. Although **22** proved comparable to **4** with calf thymus DNA, both **21** and **22** were substantially less effective at binding with 5′-(GCATGC)$_2$. This suggests that the quinoline-2-carboxylate linkage conveys a significant amount of the sandramycin selectivity for the 5′- CAT sequence which in turn is lost with the isoquinoline-1- or -3-carboxylate linkage even though high affinity binding with calf thymus DNA is maintained. Since the binding affinities of **21** and **22** are comparable to that of the mono-intercalator **24**, it also suggests they may simply be acting as mono-intercalators. Although we were not able to accurately assess the DNA binding affinity of **5**, **7**, **18** or **19** because of their limited solubility and **9–10** because of their lack of fluorescence, the attempted measurements with **5** and **7** revealed they were substantially less effective than all agents in the series indicating that the quinoline nitrogen is important for high affinity binding.

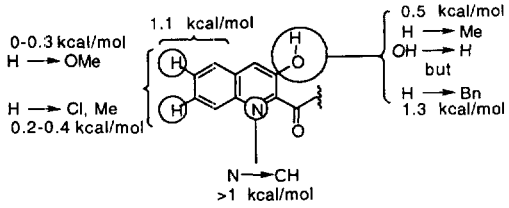

Fig. 5.

The binding of sandramycin to five self-complementary deoxyoligonucleotides is summarized in Table 3. Using the fluorescence quenching to measure of binding and the curve fitting analysis [21] of the data, sandramycin was found to bind to 5′-(GCATGC)$_2$ more effectively than the remaining four deoxyoligonucleotides. In each case, Scatchard plots revealed a 1:1 stoichiomety for the high affinity binding event. This proved consistent with expectations based on the bis-intercalation complex of sandramycin sandwiching the central two AT base-pairs of 5′-(GCATGC)$_2$ defined by ^{1}H NMR [6]. However, the distinctions were small and high affinity binding was observed with all five deoxyoligonucleotides. The two highest affinity sequences, 5′-(GCATGC)$_2$ and 5′-d(GCGCGC)$_2$, constitute repeating 5′-PuPy sequences such that each intercalation event occurs at a 5′-PyPu step [23]. The highest affinity sequence of the pair constitutes the less stable duplex, contains the deeper and sterically most accessible minor groove central to the bis-intercalation site, and the ability to accept the two gly-NH/T C2 carbonyl H-bonds identified in NMR studies. The two lower affinity sequences involve intercalation at both a 5′-PyPy step and 5′-PuPu step if it occurs about the central two base-pairs. The intercalation event interrupting the 5′-PuPu step would seem energetically more costly while that interrupting the 5′-PyPy step would provide less energetic stabilization [24]. The exception to this generalization is 5′-d(CGTACG)$_2$ which differs in the full

Table 3
Sandramycin binding to deoxyoligonucleotides

Deoxyoligonucleotide	K_b (M^{-1})	$\Delta G°$ (kcal/mol)
d(GCATGC)$_2$	23.0×10^7	−11.4
d(GCGCGC)$_2$	14.5×10^7	−11.1
d(GCCGGC)$_2$	8.5×10^7	−10.8
d(GCTAGC)$_2$	8.0×10^7	−10.8
d(CGTACG)$_2$	1.6×10^7	−9.8

[a]Calculated by nonlinear fit of all sites, see text and [21].

length sequence from the other four and constitutes the reverse sequence of 5′-d(GCATGC)$_2$. This sequence has the weakest affinity of the five deoxyoligonucleotides despite the 5′-PuPy motif. The significance of these observations are not immediately interpretable but suggest that the surrounding sequence context and directional orientation can have a large impact on the observed binding affinity [24]. The affinity of sandramycin for 5′-d(GCATGC)$_2$ relative to that of the remaining four deoxyoligonucleotides and the confirmed bis-intercalation about the central 5′-AT base-pairs [6] provided the basis for its use to compare the analogs **2**–**22** (Table 2).

4. In vitro cytotoxic activity

The in vitro cytotoxic activities secured in initial studies provided the basis for examining the chromophore analogs detailed herein. These included the comparisons of luzopeptin A and sandramycin (**1**) with sandramycin bis-*O*-benzyl ether (**2**), **24** containing a single attached aromatic chromophore, and **23** lacking both aromatic chromophores (Table 4). Throughout the five cell lines, luzopeptin A and sandramycin exhibited comparable and exceptionally potent cytotoxic activity (6–0.02 nM IC_{50}). The bis benzyl ether **2** was typically 20–1000× less potent than **1**. The agent **24** possessing a single chromophore was found to be 5000–10000× less potent than **1** and the cyclic decadepsipeptide **23** lacking both chromophores was 10^5× less potent than **1**.

Table 5 summarizes the comparison of luzopeptin A, sandramycin (**1**), and **2** with the chromophore analogs **3**–**22** in the single L1210 cell line. Several trends are clear in these comparisons (Fig. 6).

4.1 C3-Hydroxy group

First, *O*-alkylation of the chromophore 3-hydroxy group typically reduced the cytotoxic potency 500–1000×. This is clear in the comparisons of both **2** and **3** with **1** (1000×), **12** with **11** (400×), **6** with **5** (> 500×), **9** with **8** (1000×), and **20** with **19** (7×). Significantly, even *O*-methylation of the sandramycin phenol (**3**) reduced the cytotoxic potency 1000× providing an agent that was equipotent with the benzyl ether **2**. Despite this substantial reduction in potency by *O*-alkylation, removal of the phenol altogether had a much more modest effect. This is clear in the comparisons of **4** with **1** (10×), **7** with **5** (2×), and **13** with **11** (10×). The exception is the comparison of **10** with **8** (1000×) where the removal of the hydroxy group had a much larger effect. In addition, **18** was found to be more potent than **19** (300×) even though the former agent lacks the hydroxyl group of **19**. Although this effect may be unique to the quinoxaline chromophore, this was also observed with **4** in additional cell lines. Thus, the removal of the chromophore phenol has only a modest effect and, in some instances, results in more potent cytotoxic activity.

Table 4
In vitro cytotoxic activity:[a] key substructure analogs

Agent	IC_{50}, nM				
	L1210	Molt-4	786-0	Ovcar-3	B-16
Luzopeptin A	0.02	0.08	0.2	6	0.07
Sandramycin (**1**)	0.02	0.08	4	2	0.4
2	20–2	4	120	60	8
24	500	400	nt	nt	nt
23	10^5	10^5	80000	80000	nt

[a]L1210 (mouse leukemia), Molt-4 (human T-cell leukemia), 786-0 (human perirenal cell carcinoma), Ovcar-3 (human ovarian carcinoma), B-16 (melanoma).

Table 5
In vitro cytotoxic activity, L1210 (IC_{50}, nM)

1 (sandramycin)	0.02
2	20
3	20
4	0.2
5	200
6	> 10^5
7	400
8	80
9	80000
10	80000
11	0.04
12	15
13	0.4
14	0.02
16	0.01
18	3
19	1000
20	7000
21	20
22	20

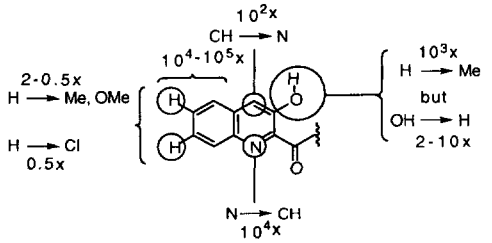

Fig. 6. Structural change impact on cytotoxic activity, rel IC_{50} indicated for removal or alteration.

4.2 Quinoline nitrogen (N1)

The quinoline nitrogen proved especially important and its removal resulted in a substantial loss of cytotoxic potency (10^4–10^3×). This is clear in the comparisons of **5** with **1** (10000×), **7** with **4** (2000×) and **6** with **2** (> 5000×).

4.3 Extended chromophore: pyridine versus quinoline

The quinoline versus pyridine comparisons embodied in **8** versus **1** (4000×), **9** versus **2** (4000×) and **10** versus **4** (4×10^5) clearly highlight the importance of the fused benzene ring (10^4–10^5×).

4.4 Quinoline versus isoquinoline

The analogous comparisons of **21** and **22** with **4** highlight the optimal quinoline-2-carboxylic acid linkage versus isoquinoline-3-carboxylic or isoquinoline-1-carboxylic acid linkage (100×). However, both **21** and **22** were 4000× (10^3–10^4×) more effective than pyridine-2-carboxylic acid (**10**) illustrating that both are more effective than might be initially anticipated.

4.5 Quinoline substitution

The incorporation of the luzopeptin chromophore into the sandramycin structure had no impact on the cytotoxic potency (**11** versus **1**, 2×) and simply constitutes the introduction of a quinoline C6 methoxy substituent. An analogous comparison of **13** with **4** (2×) and **12** with **2** (0.8×) indicates that the relative lack of impact of the introduction of the C6 methoxy group is general and that it has little effect on the cytotoxic potency of the resulting agent. The addition comparisons of **14** (1×) and **16** (0.5×) with **1** illustrate that the analogous introductions of a C6 methyl group or C7 chlorine substituent maintain or perhaps enhance the cytotoxic potency, respectively. Clear from the comparisons, is the relatively small impact of C6 and C7 substituents regardless of their electronic and steric features, at least within the limited range examined. This series of agents including **11**, **14**, and **16** constitute exceptionally potent cytotoxic agents worthy of more detailed examination. Similarly, **4** and **13** possess a level of cytotoxic potency against L1210 and chemical properties (nonacidic) that make them alternative and attractive agents for further examination.

4.6 Quinoxaline versus quinoline

Finally, **18** which incorporates the echinomycin chromophore and is analogous to that found in the recently isolated quinoxapeptins lacking only the C6 methoxy group proved to be approximately 100× less potent than **1** and approximately 10× less potent than **4** and **13**.

Thus, sandramycin was found to be equipotent to luzopeptin A, the most potent member of the luzopeptins. Removal of the C3 hydroxy group has only a small effect (2–10×) while its conversion to a methyl or benzyl ether has a pronounced diminishing effect (1000×) (Fig. 6). One of the largest effects observed was removal of the chromophore nitrogen which reduced the

Table 6
In vitro cytotoxic activity, IC_{30} (nM)

Cell line (tumor type)	Luzopeptin A	Sandramycin	**4**
L1210 (mouse leukemia)	0.02	0.02	0.2
Molt-4 (human T-cell leukemia)	0.7	0.7	3
HL-60 (human promyelomic leukemia)	0.2	80	0.001
	luzopeptin A = sandramycin > **4**		
B16 (melanoma)	0.06	0.4	0.06
SK-MEL28 (human melanoma)	0.0005	1	0.001
M24-MET (human metastatic melanoma)	0.02	0.4	0.04
	4 = luzopeptin A > sandramycin		
BT-549 (human breast carcinoma)	0.5	1	0.01
MCF-7 (human breast carcinoma)	20	300	0.04
OVCAR-3 (human ovarian carcinoma)	6	4	1
PC-3 (human prostate carcinoma)	0.09	0.2	0.001
SIHA (human squamous cervix carcinoma)	0.005	0.3	0.001
786-0 (human perirenal cell carcinoma)	0.02	8	0.01
	4 > luzopeptin A > sandramycin		
H322 (human lung adenocarcinoma)	10	20	10
UCLA-P3 (human lung adenocarcinoma)	2	10	0.002
HT-29 (human colon adenocarcinoma)	0.5	1	0.01
	4 > luzopeptin A > sandramycin		
U251 (human CNS cancer)	0.9	6	0.001

cytotoxic potency 10000×. Substitution of a pyridine versus quinoline chromophore reduced the potency by approximately 1000× and the use of the isomeric 1- or 3-isoquinoline chromophore reduced the potency by approximately 100× relative to 2-quinoline. Interestingly, incorporation of the echinomycin chromophore provided agents 100× less potent while incorporation of the luzopeptin chromophore provided agents equipotent with sandramycin. Importantly, the nature of the C6 or C7 chromophore substituents had essentially no effect on the cytotoxic properties of the agents.

In order to establish the role and subtle importance of the key substituents more carefully, a detailed comparison of luzopeptin A, sandramycin (**1**) and **4** was conducted (Table 6). Several interesting observations were made in these additional comparisons. In the leukemia cell lines, typically it was found that luzopeptin A and sandramycin were equipotent and more potent than **4** with one notable exception where **4** was found to be exceptionally potent (HL-60). In the remaining cell lines, **4** proved to be equipotent or more potent than either luzopeptin A and sandramycin: carcinomas and adenocarcinomas, **4** > luzopeptin A > sandramycin (**1**); melanomas, **4** = luzopeptin A > sandramycin (**1**). Thus, the removal of the acidic phenol from the chromophore of sandramycin providing **4** afforded an agent that typically exhibits more potent cytotoxic activity in a range of cell lines. In many instances, the cytotoxic potency of **4** is exceptional and it was found to typically exhibit IC_{50} values in the range of 200–1 pM. This places it among the most potent agents defined to date.

5. Inhibition of HIV-1 reverse transcriptase

Sandramycin and its analogs were also examined for their ability to inhibit HIV-1 reverse transcriptase analogous to the quinoxapeptins and luzopeptin A [5,13,25]. In these prior studies, quinoxapeptin A and luzopeptin A exhibited comparable inhibitory potency while quinoxapeptin B was approximately 2× less potent. All three were several orders of magnitude more potent (5000×) than the most potent natural products defined in a screen of > 150 candidate natural products [13,25]. Moreover, quinoxapeptin A was found to be nearly equally effective (1–3×) against two single mutant and one double mutant of HIV-1 reverse transcriptase by a mechanism that involves template-primer binding and noncompetitive enzyme inhibition [5]. Thus, their use in combination with non-nucleoside inhibitors subject to mutation resistance may prove especially important.

The assay was performed following a slight modification of an established procedure [26] and the results are summarized in Table 7. Sandramycin proved slightly more effective than luzopeptin A and both exhibit IC_{50} values of 130–190 nM. For luzopeptin A, this is 20–30× higher than values reported elsewhere (7 nM) and may be attributed to differences in the assay. A similar potency was observed with **11** which incorporates the luzopeptin chromophore into the sandramycin structure. Comparable but slightly less potent inhibition was observed with **4**, **13**, **14**, **16**, and **18**. Within this potent series, the agents possessing a C3 phenol were found to be 3–6× more potent than the corresponding agents lacking the phenol (C3-H). Interestingly, the analog **18**, which incorporates the echinomycin chromophore, and **4** proved equipotent and only 3× less potent than sandramycin itself. *O*-Alkylation of the C3 phenol with **3** and **17** resulted in a marked reduction in the inhibitory potency and the extent of the reduction (10× versus > 500×) correlates with the size of the substituent and its relative effect on DNA binding affinity. The alternative analogs **5**, **7**, **8**, **10**, **21**, and **22** were much less effective and follow affinity trends established in the DNA binding studies. These results are summarized in Fig. 7. Because of their differential cytotoxicity (**18** < **1**, 150×; **3** < **1**, 1000×) but their maintained ability to

Table 7
Inhibition of HIV-1 reverse transcriptase

Inhibitor	IC_{50} (μM)
Luzopeptin A	0.19
Sandramycin (**1**)	0.13
3	1.0
4	0.48
5	13.0
7	> 200
8	79
10	> 100
11	0.11
13	0.70
14	0.70
16	0.35
17	> 100
18	0.44
21	> 100
22	> 100

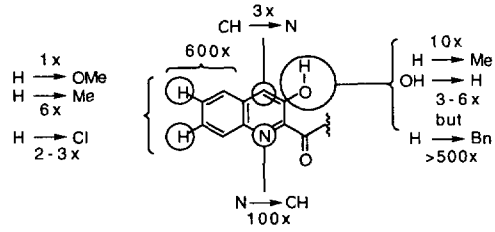

Fig. 7. Structural change impact on RT inhibition, rel IC_{50} indicated for removal or alteration.

inhibit HIV-1 reverse transcriptase, both **3** and **18** merit further examination.

6. Conclusions

The synthesis of a series of analogs of sandramycin (**1**) was accomplished by the penultimate introduction of substitution chromophores on the key intermediate **23**. Each analog contained a deep-seated structural change in the chromophore including the deletion of key functional groups or core structural elements capable of revealing its role in the high affinity bis-intercalation binding of sandramycin.

Fluorescence quenching studies were employed to establish the DNA binding affinity of sandramycin and the chromophore analogs **2–24** for calf thymus DNA and 5′-d(GCXXGC)$_2$ where XX = AT, TA, GC, and CG. With the latter studies, the determination of absolute binding constants within a single high affinity bis-intercalation site permitted a quantitative assessment of the sequence selectivity of sandramycin (**1**) as 5′-d(GCATGC)$_2$ > 5′-d(GCGCGC)$_2$, $\Delta\Delta G^\circ = 0.3$ kcal/mol > 5′-d(GCTAGC)$_2$, 5′-d(GCCGGC), $\Delta\Delta G^\circ = 0.6$ kcal/mol and a quantitative assessment of the chromophore structural features contributing to binding at a single high affinity bis-intercalation site. The two highest affinity sequences constitute repeating 5′-PuPy motifs with each intercalation event occurring at a 5′-PyPu step. The highest affinity sequence of the pair constitutes the less stable duplex, possesses the sterically most accessible minor groove central to the bis-intercalation site, and the ability to accept the two gly-NH/T C2 carbonyl H-bonds identified in NMR studies. Whether these features, or more subtle features, are responsible for the binding preference will be the subject of continued examination. The chromophore nitrogen inherent in the quinoline-2-carboxylate structure is essential for binding affinity (> 1 kcal/mol per chromophore), the fused benzene ring contributes substantially (ca. 1.1 kcal/mol per chromophore) while the C3 phenol only slightly enhances binding (0.5 kcal/mol per chromophore). The addition of C6 or C7 substituents only slightly diminishes binding affinity and the luzopeptin chromophore incorporating a C6 methoxy substituent was established to be slightly less effective than the sandramycin chromophore. These studies suggest substantial modifications may be made at both the C6 and C7 positions without adversely affecting binding affinity but none to date have been observed to enhance binding.

To a first approximation, the cytotoxic properties of the agents and their ability to inhibit HIV-1 reverse transcriptase were found to follow trends established in the DNA binding affinities. The exception to this generalization was **4** which lacks the chromophore phenol. Although it was found to be typically 4–10× less potent than luzopeptin A or sandramycin against leukemia cell lines, it proved to be equipotent or more potent against melanomas, carcinomas, and adenocarcinomas. In these latter tumor types, it was found to exhibit cytotoxic potencies ranging from 1 pM to 10 nM which was 1–10,000× more potent than luzopeptin A or sandramycin placing it among the most potent agents identified to date. Although many explanations may account for such observations, one of the most obvious is that the removal of the acidic phenol may lead to better target delivery without adversely affecting the DNA binding affinity or selectivity.

7. Experimental

*7.1 General procedure for the coupling of chromophore carboxylic acids with 23: (*N-*(3-Benzyloxy-6-methoxyquinolinyl-2-carbonyl)*-D-*Ser-Pip-Gly-Sar-NMe-Val)$_2$ (serine hydroxyl) dilactone (12)*

A solution **23** [6] (18.8 mg, 0.017 mmol) in 3 M HCl–EtOAc (1 ml) at 25 °C was stirred for 30 min. The solvent was removed in vacuo to afford the hydrochloride salt **25** (17.1 mg, 16.6 mg theoretical, 100%) as a white powder which was used directly in the next reaction.

A solution of the hydrochloride salt **25** (16.6 mg, 0.017 mmol) and 3-benzyloxy-6-methoxyquinoline-2-carboxylic acid [15] (21.5 mg, 0.07 mmol, 4.0 equiv.) in DMF (2 ml) was treated sequentially with $NaHCO_3$ (14.6 mg, 0.17 mmol, 10.0 equiv.), HOBt (14.1 mg, 0.10 mmol, 6.0 equiv.), and EDCI (13.4 mg, 0.07 mmol, 4.0 equiv.) and the reaction mixture was stirred at 25 °C for 72 h. The reaction mixture was diluted with EtOAc (20 ml) and washed with H_2O (10 ml), saturated aqueous NaCl (10 ml), dried (Na_2SO_4), filtered, and concentrated in vacuo. Flash chromatography (SiO_2, 1 × 16 cm, 0–5% EtOH–CH_2Cl_2 gradient) afforded **12** (20.6 mg, 25.5 mg theoretical, 81%) as a white powder: $R_f = 0.58$ (20% CH_3CN–EtOAc); $[\alpha]_D^{23}$ −113 (*c* 0.2, $CHCl_3$); ^{1}H NMR ($CDCl_3$, 400 MHz) δ 9.04 (d, 2H, $J = 6.3$ Hz, Ser-NH), 8.48 (d, 2H, $J = 4.4$ Hz, Gly-NH), 7.80 (d, 2H, $J = 9.2$ Hz, C8′-H), 7.55 (d, 4H, $J = 7.3$ Hz, phenyl C2 and C6-H), 7.49 (s, 2H, C4′-H), 7.39 (t, 4H, $J = 7.3$ Hz, phenyl C3 and C5-H), 7.29 (t, 2H, $J = 7.3$ Hz, phenyl C4-H), 7.19 (dd, 2H, $J = 2.7$, 9.2 Hz, C7′-H), 6.92 (d, 2H, $J = 2.7$ Hz, C5′-H), 5.46 (d, 2H, $J = 4.1$ Hz, Pip-α-CH), 5.44 (d, 2H, $J = 16.6$ Hz, Sar-α-CH), 5.31 (m, 6H, $PhCH_2$ and Ser-α-CH), 4.85 (dd, 2H, $J = 1.4$, 11.5 Hz, Ser-β-CH), 4.82 (d, 2H, $J = 11$ Hz, Val-α-CH), 4.57 (dd, 2H, $J = 2.5$, 11.5 Hz, Ser-β-CH), 4.42 (dd, 2H, $J = 5.7$, 18.2 Hz, Gly-α-CH), 4.03 (d, 2H, $J = 18.2$ Hz, Gly-α-CH), 3.99 (m, 2H, Pip-ε-CH), 3.90 (s, 6H, OCH_3), 3.76 (d, 2H, $J = 13.2$ Hz, Pip-ε-CH), 3.46 (d, 2H, $J = 16.6$ Hz, Sar-α-CH), 3.07 (s, 6H, Val-NCH_3), 2.91 (s, 6H, Sar-NCH_3), 2.06 (d split septet, 2H, $J = 6.5$, 11.0 Hz, Val-β-

CH), 1.80–1.45 (m, 12H, Pip-$(CH_2)_3$), 0.94 (d, 6H, J=6.5 Hz, Val-γ-CH_3), 0.80 (d, 6H, J=6.5 Hz, Val-γ-CH_3); ^{13}C NMR ($CDCl_3$, 100 MHz) δ 172.7, 169.2, 169.1, 167.7, 167.1, 163.5, 159.4, 152.3, 139.5, 137.7, 136.1, 131.8, 131.0, 128.7, 127.9, 126.8, 120.7, 116.3, 103.6, 70.8, 62.9, 62.3, 55.6, 52.4, 50.7, 49.3, 43.8, 41.9, 34.9, 30.4, 28.7, 26.5, 24.8, 20.2, 19.4, 19.0; IR (KBr) ν_{max}, 3487, 3327, 2936, 1742, 1672, 1638, 1492, 1417, 1263, 1229, 1136, 1019, 832, 734 cm^{-1}; FABHRMS (NBA) m/z 1461.6770 ($M+H^+$, $C_{76}H_{92}N_{12}O_{18}$ requires 1461.6731).

*7.2 General procedure for bis O-benzyl ether deprotection: (*N*-(3-hydroxy-6-methoxyquinolinyl-3-carbonyl)-*D*-Ser-Pip-Gly-Sar-NMe-Val)$_2$ (serine hydroxyl) dilactone (**11**)*

A sample of 10% Pd–C (3 mg) was added to a solution of **12** (14.3 mg, 0.0098 mmol) in EtOAc (4 ml) and the black suspension was stirred at 25 °C under an atmosphere of H_2 (1 atm) for 14 h. The catalyst was removed by filtration through Celite and the filtrate was concentrated in vacuo. Flash chromatography (SiO_2, 1×16 cm, EtOAc eluent) afforded **11** (10.2 mg, 12.5 mg theoretical, 82%) as a white powder: R_f = 0.31 (EtOAc); $[\alpha]_D^{23}$ −118 (*c* 0.28, $CHCl_3$); ^1H NMR ($CDCl_3$, 400 MHz) δ 11.76 (s, 2H, OH), 9.44 (d, 2H, J=5.0 Hz, Ser-NH), 8.52 (br s, 2H, Gly-NH), 7.68 (d, 2H, J=8.5 Hz, C7-H), 7.48 (s, 2H, C4-H), 7.14 (d, 2H, J=8.5 Hz, C8-H), 6.90 (d, 2H, J=2.7 Hz, C5-H), 5.56 (d, 2H, J=5.9 Hz, Pip-α-CH), 5.53 (d, 2H, J=16.5 Hz, Sar-α-CH), 5.25 (d, 2H, J=5.0 Hz, Ser-α-CH), 4.96 (d, 2H, J=11.7 Hz, Ser-β-CH), 4.87 (d, 2H, J=11.0 Hz, Val-α-CH), 4.43 (d, 4H, J=11.7 Hz, Ser-β-CH and Gly-α-CH), 4.05 (m, 4H, Gly-α-CH and Pip-ε-CH), 3.92 (s, 6H, OCH_3), 3.74 (m, 2H, Pip-ε-CH), 3.54 (d, 2H, J=16.5 Hz, Sar-α-CH), 3.10 (s, 6H, Val-NCH_3), 2.93 (s, 6H, Sar-NCH_3), 2.04 (d split septet, 2H, J=11.0, 6.5 Hz, Val-β-CH), 1.80–1.50 (m, 12H, Pip-$(CH_2)_3$), 0.93 (d, 6H, J=6.5 Hz, Val-γ-CH_3), 0.79 (d, 6H, J=6.5 Hz, Val-γ-CH_3); ^{13}C NMR ($CDCl_3$, 100 MHz) δ 172.6, 169.4, 169.2, 168.0, 167.7, 166.3, 159.5, 154.4, 137.8, 133.4, 132.1, 130.9, 121.0, 1 18.9, 103.0, 62.4, 62.0, 55.6, 52.5, 50.5, 49.3, 43.9, 41.9, 34.9, 30.3, 28.7, 26.3, 24.9, 20.2, 19.4, 18.7; IR (KBr) ν_{max} 3330, 2936, 1745, 1668, 1640 cm^{-1}; FABHRMS (NBA) m/z 1281.5890 ($M+H^+$, $C_{62}H_{80}N_{12}O_{18}$ requires 1281.5792).

*7.2.1 (*N*-(3-Methoxyquinolinyl-2-carbonyl)-*D*-Ser-Pip-Gly-Sar-NMe-Val)$_2$ (serine hydroxyl) dilactone (**3**)*

0.0093 mmol scale; flash chromatography (SiO_2, 1×16 cm, 0–5% EtOH–CH_2Cl_2 gradient) afforded **3** (9.7 mg, 11.6 mg theoretical, 84%) as white powder: R_f = 0.49 (5% EtOH–CH_2Cl_2); $[\alpha]_D^{23}$ −136 (*c* 0.2, $CHCl_3$); ^1H NMR ($CDCl_3$, 400 MHz) δ 9.02 (d, 2H, J=6.2 Hz, Ser-NH), 8.48 (d, 2H, J=4.2 Hz, Gly-NH), 7.96 (m, 2H, C5′-H), 7.74 (m, 2H, C8′-H), 7.57 (s, 2H, C4′-H), 7.56 (m, 4H, C6′ and C7′-H), 5.46 (d, 2H, J=16.5 Hz, Sar-α-CH), 5.45 (d, 2H, J=7.3 Hz, Pip-α-CH), 5.31 (d, 2H, J=6.2 Hz, Ser-α-CH), 4.86 (dd, 2H, J=1.8, 12.0 Hz, Ser-β-CH), 4.83 (d, 2H, J=11.0 Hz, Val-α-CH), 4.57 (dd, 2H, J=2.8, 12.0 Hz, Ser-β-CH), 4.42 (dd, 2H, J=5.7, 18.3 Hz, Gly-α-CH), 4.06 (m, 2H, Gly-α-CH), 4.03 (s, 6H, OCH_3), 4.01 (m, 2H, Pip-ε-CH), 3.76 (d, 2H, J=14.0 Hz, Pip-ε-CH), 3.49 (d, 2H, J=16.5 Hz, Sar-α-CH), 3.09 (s, 6H, Val-NCH_3), 2.92 (s, 6H, Sar-NCH_3), 2.07 (d split septet, 2H, J=6.5, 11.0 Hz, Val-β-CH), 1.80–1.45 (m, 12H, Pip-$(CH_2)_3$), 0.95 (d, 6H, J=6.5 Hz, Val-γ-CH_3), 0.81 (d, 6H, J=6.5 Hz, Val-γ-CH_3); ^{13}C NMR ($CDCl_3$, 100 MHz) δ 172.6, 169.3, 169.2, 167.7, 167.0, 163.5, 152.9, 141.9, 141.5, 130.3, 129.6, 128.5, 127.4, 126.3, 115.1, 62.8, 62.1, 56.1, 52.5, 50.8, 49.3, 43.9, 41.9, 34.9, 30.4, 28.7, 26.5, 24.8, 20.2, 19.4, 19.0; IR (KBr) ν_{max} 3324, 2939, 1741, 1672, 1636, 1491, 1467, 1417, 1344, 1286, 1201, 1137, 1097, 1013 cm^{-1}; FABHRMS (NBA) m/z 1249.5961 ($M+H^+$, $C_{62}H_{80}N_{12}O_{16}$ requires 1249.5894).

*7.2.2 (*N*-(Quinolinyl-2-carbonyl)-*D*-Ser-Pip-Gly-Sar-NMe-Val)$_2$ (serine hydroxyl) dilactone (**4**)*

0.0056 mmol scale; flash chromatography (SiO_2, 1×16 cm, 0–10% EtOH–CH_2Cl_2 gradient) afforded **4** (5.2 mg, 6.7 mg theoretical, 78%) as white powder: R_f = 0.38 (10% CH_3CN–EtOAc); $[\alpha]_D^{23}$ −139 (*c* 0.3, $CHCl_3$); ^1H NMR ($CDCl_3$, 400 MHz) δ 9.42 (d, 2H, J=6.3 Hz, Ser-NH), 8.53 (d, 2H, J=4.6 Hz, Gly-NH), 8.29 (s, 4H, C3′ and C4′-H), 7.97 (d, 2H, J=8.3 Hz, C5′-H), 7.87 (dd, 2H, J=1.0, 8.3 Hz, C8′-H), 7.72 (ddd, J=1.4, 7.1, 8.3 Hz, C7′-H), 7.60 (ddd, 2H, J=1.0, 7.1, 8.3 Hz, C6′-H), 5.56 (d, 2H, J=7.1 Hz, Pip-α-CH), 5.55 (d, 2H, J=16.3 Hz, Sar-α-CH), 5.31 (d, 2H, J=6.3 Hz, Ser-α-CH), 4.97 (dd, 2H, J=1.5, 12.0 Hz, Ser-β-CH), 4.86 (d, 2H, J=11.0 Hz, Val-α-CH), 4.46 (dd, 2H, J=2.9, 12.0 Hz, Ser-β-CH), 4.43 (dd, 2H, J=4.5, 12.8 Hz, Gly-α-CH), 4.08 (m, 2H, Pip-ε-CH), 4.04 (d, 2H, J=16.8 Hz, Gly-α-CH), 3.76 (d, 2H, J=13.3 Hz, Pip-α-CH), 3.55 (d, 2H, J=16.3 Hz, Sar-α-CH), 3.14 (s, 6H, Val-NCH_3), 2.93 (s, 6H, Sar-NCH_3), 2.03 (d split septet, 2H, J=6.6, 11.0 Hz, Val-β-CH), 1.82–1.52 (m, 12H, Pip-$(CH_2)_3$), 0.92 (d, 6H, J=6.6 Hz, Val-γ-CH_3), 0.78 (d, 6H, J=6.5 Hz, Val-γ-CH_3); ^{13}C NMR ($CDCl_3$, 100 MHz) δ 172.7, 169.3, 169.1, 167.7, 166.9, 163.8, 149.4, 146.6, 137.3, 129.9,129.7, 129.4, 128.7,127.8, 118.8, 62.7, 62.0, 52.4, 50.8, 49.3, 43.8, 41.9, 34.9, 30.4, 28.8, 26.3, 24.9, 20.2, 19.4, 18.8; IR (KBr) ν_{max} 3328, 2939, 1743, 1669, 1636, 1497, 1425, 1286, 1136, 1015, 847, 777 cm^{-1}; FABHRMS (NBA) m/z 1189.5685 ($M+H^+$, $C_{60}H_{76}N_{12}O_{14}$ requires 1189.5682).

*7.2.3 (*N*-(3-Benzyloxynaphthyl-2-carbonyl)-*D*-Ser-Pip-Gly-Sar-NMe-Val)$_2$ (serine hydroxyl) dilactone (**6**)*

0.015 mmol scale; flash chromatography (SiO_2, 1×16 cm, 0–5% EtOH–CH_2Cl_2 gradient) afforded **6**

(18.5 mg, 21.7 mg theoretical, 85%) as white powder: $R_f = 0.36$ (20% CH_3CN–EtOAc); $[\alpha]_D^{23}$ −64 (*c* 0.6, $CHCl_3$); ^1H NMR ($CDCl_3$, 400 MHz) δ 9.32 (d, 2H, $J = 5.8$ Hz, Ser-NH), 8.76 (s, 2H, C1′-H), 8.47 (d, 2H, $J = 3.8$ Hz, Gly-NH), 7.88 (d, 2H, $J = 8.1$ Hz, C5′-H), 7.62 (d, 2H, $J = 8.1$ Hz, C8′-H), 7.50–7.25 (m, 14H, C6′, C7′, and phenyl CH), 7.19 (s, 2H, C4′-H), 5.48–5.35 (m, 8H, Pip-α-CH, Ser-α-CH, and $PhCH_2$), 5.24 (d, 2H, $J = 16.6$ Hz, Sar-α-CH), 4.75 (d, 2H, $J = 11.0$ Hz, Val-α-CH), 4.74 (dd, 2H, $J = 3.1$, 11.7 Hz, Ser-β-CH), 4.63 (dd, 2H, $J = 3.1$, 11.7 Hz, Ser-β-CH), 4.41 (dd, 2H, $J = 5.5$, 18.3 Hz, Gly-α-CH), 4.09 (d, 2H, $J = 18.3$ Hz, Gly-α-CH), 3.98 (m, 2H, Pip-ε-CH), 3.76 (d, 2H, $J = 12.8$ Hz, Pip-ε-CH), 3.24 (d, 2H, $J = 16.6$ Hz, Sar-α-CH), 2.90 (s, 6H, Val-NCH_3), 2.88 (s, 6H, Sar-NCH_3), 1.98 (d split septet, 2H, $J = 6.5$, 11.0 Hz, Val-β-CH), 1.75–1.40 (m, 12H, Pip-$(CH_2)_3$), 0.92 (d, 6H, $J = 6.5$ Hz, Val-γ-CH_3), 0.74 (d, 6H, $J = 6.5$ Hz, Val-γ-CH_3); ^{13}C NMR ($CDCl_3$, 100 MHz) δ 172.8, 169.3, 169.2, 167.6, 166.7, 164.4, 154.1, 136.1, 135.6, 133.9, 129.1, 128.7, 128.3, 128.2, 128.0, 127.0, 126.2, 124.7, 122.5, 108.8, 71.2, 63.2, 62.2, 52.3, 51.4, 49.2, 43.9, 42.0, 34.9, 30.0, 28.8, 26.5, 24.8, 20.3, 19.4, 18.9; IR (KBr) ν_{max} 3329, 2939, 1742, 1639, 1595, 1498, 1455, 1416, 1355, 1259, 1224, 1135, 1076, 1016, 920, 835, 732 cm^{-1}; FABHRMS (NBA) *m/z* 1399.6622 ($M + H^+$, $C_{76}H_{90}N_{10}O_{16}$ requires 1399.6615).

7.2.4 (N-(Naphthyl-2-carbonyl)-D-Ser-Pip-Gly-Sar-NMe-Val)$_2$ (serine hydroxyl) dilactone (7)

0.0095 mmol scale; flash chromatography (SiO_2, 1×16 cm, 0–5% EtOH–CH_2Cl_2 gradient) afforded **7** (10.3 mg, 11.3 mg theoretical, 91%) as white powder: $R_f = 0.24$ (50% CH_3CN–EtOAc); $[\alpha]_D^{23}$ −101 (*c* 0.34, $CHCl_3$); ^1H NMR ($CDCl_3$, 400 MHz) δ 8.56 (d, 2H, $J = 4.3$ Hz, Ser-NH), 8.33 (s, 2H, C1-H), 7.90 (d, 2H, $J = 4.3$ Hz, Gly-NH), 7.86 (d, 4H, $J = 8.8$ Hz, C5 and C8-H), 7.84 (dd, 2H, $J = 8.9$, 1.6 Hz, C3-H), 7.54 (m, 4H, C6 and C7-H), 5.39 (d, 2H, $J = 16.5$ Hz, Sar-α-CH), 5.38 (d, 2H, $J = 4.9$ Hz, Pip-α-CH), 5.32 (m, 2H, $J = 16.5$ Hz, Ser-α-CH), 4.83 (d, 2H, $J = 11.0$ Hz, Val-α-CH), 4.81 (d, 2H, $J = 11.8$ Hz, Ser-β-CH), 4.64 (dd, 2H, $J = 11.8$, 3.2 Hz, Ser-β-CH), 4.45 (dd, 2H, $J = 18.3$, 5.8 Hz, Gly-α-CH), 4.06 (d, 2H, $J = 18.3$ Hz, Gly-α-CH), 4.00 (m, 2H, Pip-ε-CH), 3.77 (m, 2H, Pip-ε-CH), 3.47 (d, 2H, $J = 16.5$ Hz, Sar-α-CH), 2.99 (s, 6H, Val-NCH_3), 2.94 (s, 6H, Sar-NCH_3), 2.08 (d split septet, 2H, $J = 6.5$, 11.0 Hz, Val-β-CH), 1.80–1.45 (m, 12H, Pip$(CH_2)_3$), 0.95 (d, 6H, $J = 6.5$ Hz, Val-γ-CH_3), 0.81 (d, 6H, $J = 6.5$ Hz, Val-γ-CH_3); ^{13}C NMR ($CDCl_3$, 100 MHz) δ 172.6, 169.3, 169.2, 167.6, 167.2, 166.4, 134.8, 132.6, 131.1, 129.0, 128.5, 127.7, 127.6, 126.7, 123.5, 63.1, 62.2, 52.7, 51.1, 49.3, 44.0, 41.9, 35.0, 30.1, 29.7, 28.5, 26.6, 24.7, 20.1, 19.3, 18.9; IR (KBr) ν_{max} 3322, 2939, 1737, 1639, 1491, 1452, 1413, 1290, 1133, 1098, 1015, 916, 730 cm^{-1}; FABHRMS (NBA) *m/z* 1187.5779 ($M + H^+$, $C_{62}H_{78}N_{10}O_{14}$ requires 1187.5777).

7.2.5 (N-(3-Benzyloxypyridyl-2-carbonyl)-D-Ser-Pip-Gly-Sar-NMe-Val)$_2$ (serine hydroxyl) dilactone (9)

0.0117 mmol scale; flash chromatography (SiO_2, 1×16 cm, 0–5% EtOH–CH_2Cl_2 gradient) afforded **9** (13.0 mg, 15.2 mg theoretical, 85%) as white powder: $R_f = 0.4$ (5% EtOH–CH_2Cl_2); $[\alpha]_D^{23}$ −64 (*c* 0.13, $CHCl_3$); ^1H NMR ($CDCl_3$, 400 MHz) δ 9.04 (d, 2H, $J = 5.8$ Hz, Ser-NH), 8.47 (d, 2H, $J = 4.6$ Hz, Gly-NH), 8.17 (dd, 2H, $J = 1.2$, 4.2 Hz, C6′-H), 7.50–7.26 (m, 14H, C4′, C5′, and phenyl CH), 5.40 (d, 2H, $J = 16.5$ Hz, Sar-α-CH), 5.31–5.20 (m, 6H, $PhCH_2$ and Ser-α-CH), 4.81 (d, 2H, $J = 11.0$ Hz, Val-α-CH), 4.78 (d, 2H, $J = 12.0$ Hz, Ser-β-CH), 4.58 (dd, 2H, $J = 2.7$, 12.0 Hz, Ser-β-CH), 4.41 (dd, 2H, $J = 5.8$, 18.3 Hz, Ser-β-CH), 4.01 (d, 2H, $J = 18.3$ Hz, Ser-β-CH), 3.98 (m, 2H, Pip-ε-CH), 3.74 (d, 2H, $J = 13.8$ Hz, Pip-ε-CH), 3.41 (d, 2H, $J = 16.5$ Hz, Sar-α-CH), 2.97 (s, 6H, Val-NCH_3), 2.91 (s, 6H, Sar-NCH_3), 2.06 (d split septet, 2H, $J = 6.5$, 11.0 Hz, Val-β-CH), 1.80–1.42 (m, 12H, Pip-$(CH_2)_3$), 0.95 (d, 6H, $J = 6.5$ Hz, Val-γ-CH_3), 0.80 (d, 6H, $J = 6.5$ Hz, Val-γ-CH_3); ^{13}C NMR ($CDCl_3$, 100 MHz) δ 172.7, 169.3, 169.2, 167.7, 167.0, 163.4, 155.0, 140.8, 139.0, 135.9, 128.7, 128.0, 127.8, 126.9, 122.9, 71.0, 63.1, 62.2, 52.4, 50.6, 49.3, 43.8, 41.9, 34.9, 30.3, 28.7, 26.6, 24.8, 20.2, 19.4, 19.0; IR (KBr) ν_{max} 3326, 2930, 1741, 1669, 1638, 1494, 1454, 1288, 1136, 1017, 739, 698 cm^{-1}; FABHRMS (NBA-CsI) *m/z* 1433.5160 ($M + Cs^+$, $C_{66}H_{84}N_{12}O_{16}$ requires 1433-5183).

7.2.6 (N-(Pyridyl-2-carbonyl)-D-Ser-Pip-Gly-Sar-NMe-Val)$_2$ (serine hydroxyl) dilactone (10)

0.0076 mmol scale; flash chromatography (SiO_2, 1×16 cm, 0–10% EtOH–CH_2Cl_2 gradient) afforded **10** (7.8 mg, 8.3 mg theoretical, 94%) as white powder: $R_f = 0.6$ (10% EtOH–CH_2Cl_2); $[\alpha]_D^{23}$ −103 (*c* 0.35, $CHCl_3$); ^1H NMR ($CDCl_3$, 400 MHz) δ 9.23 (d, 2H, $J = 6.4$ Hz, Ser-NH), 8.50 (m, 4H, Gly-NH and C5-H), 8.17 (d, 2H, $J = 7.8$ Hz, C3-H), 7.82 (ddd, 2H, $J = 1.7$, 7.6, 7.7 Hz, C4-H), 7.39 (ddd, 2H, $J = 1.2$, 4.6, 7.6 Hz, C5-H), 5.47 (d, 2H, $J = 5.5$ Hz, Pip-α-CH), 5.46 (d, 2H, $J = 16.6$ Hz, Sar-α-CH), 5.24 (d, 2H, $J = 6.4$ Hz, Ser-α-CH), 4.84 (d, 4H, $J = 11.0$ Hz, Val-α-CH and Ser-β-CH), 4.49 (dd, 2H, $J = 2.8$, 11.7 Hz, Ser-β-CH), 4.42 (dd, 2H, $J = 5.8$, 18.2 Hz, Gly-α-CH), 4.02 (m, 2H, Pip-ε-CH), 4.00 (d, 2H, $J = 17.0$ Hz, Gly-α-CH), 3.73 (m, 2H, Pip-ε-CH), 3.48 (d, 2H, $J = 16.6$ Hz, Sar-α-CH), 3.03 (s, 6H, Val-NCH_3), 2.92 (s, 6H, Sar-NCH_3), 2.06 (d split septet, 2H, $J = 6.5$, 11.0 Hz, Val-β-CH), 1.78–1.45 (m, 12H, Pip-$(CH_2)_3$), 0.93 (d, 6H, $J = 6.5$ Hz, Val-γ-CH_3), 0.80 (d, 6H, $J = 6.5$ Hz, Val-γ-CH_3); ^{13}C NMR ($CDCl_3$, 100 MHz) δ 172.7, 169.3, 169.1, 167.8, 166.8, 163.8, 149.6, 148.3, 137.1, 126.2, 122.2, 62.8, 62.1, 52.4, 50.6, 49.3, 43.8, 41.8, 34.9, 30.3, 28.7, 26.4, 24.8, 20.1, 19.4, 18.8; IR (KBr) ν_{max} 3327, 2936, 1744, 1672, 1637, 1571, 1462, 1426, 1288, 1136, 1017, 918, 731 cm^{-12}; FABHRMS (NBA) *m/z* 1089–5360 ($M + H^+$, $C_{52}H_{72}N_{12}O_{14}$ requires 1089.5369).

*7.2.7 (N-(6-Methoxyquinolinyl-2-carbonyl)-D-Ser-Pip-Gly-Sar-NMe-Val)$_2$ (serine hydroxyl) dilactone (**13**)*

0.0081 mmol scale; flash chromatography (SiO_2, 1×16 cm, 0–5% EtOH–CH_2Cl_2 gradient) afforded **13** (9.0 mg, 10.1 mg theoretical, 89%) as white powder: R_f = 0.5(5% EtOH–CH_2Cl_2); $[\alpha]_D^{23}$ −122 (*c* 0.2, $CHCl_3$); ^{1}H NMR ($CDCl_3$, 400 MHz) δ 9.34 (d, 2H, *J* = 6.4 Hz, Ser-NH), 8.52 (d, 2H, *J* = 4.6 Hz, Gly-NH), 8.23 (d, 2H, *J* = 8.5 Hz, C3′-H), 8.15 (d, 2H, *J* = 8.5 Hz, C4′-H), 7.84 (d, 2H, *J* = 9.2 Hz, C8′-H), 7.36 (dd, 2H, *J* = 2.7, 9.2 Hz, C7′-H), 7.10 (d, 2H, *J* = 2.7 Hz, C5′-H), 5.55 (d, 2H, *J* = 5.4 Hz, Pip-α-CH), 5.54 (d, 2H, *J* = 16.4 Hz, Sar-α-CH), 5.30 (d, 2H, *J* = 6.4 Hz, Ser-α-CH), 4.94 (dd, 2H, *J* = 1.5, 11.0 Hz, Ser-β-CH), 4.85 (d, 2H, *J* = 11.0 Hz, Val-α-CH), 4.45 (m, 4H, Ser-β-CH, and Gly-α-CH), 4.06 (m, 4H, Gly-α-CH and Pip-ε-CH), 3.95 (s, 6H, OCH_3), 3.76 (d, 2H, *J* = 13.2 Hz, Pip-ε-CH), 3.54 (d, 2H, *J* = 16.4 Hz, Sar-α-CH), 3.13 (s, 6H, Val-NCH_3), 2.93 (s, 6H, Sar-NCH_3), 2.04 (d split septet, 2H, *J* = 6.5, 11.0 Hz, Val-β-CH), 1.82–1.50 (m, 12H, Pip-$(CH_2)_3$), 0.92 (d, 6H, *J* = 6.5 Hz, Val-γ-CH_3), 0.78 (d, 6H, *J* = 6.5 Hz, Val-γ-CH_3); ^{13}C NMR ($CDCl_3$, 100 MHz) δ 172.7, 169.3, 169.1, 167.7, 167.0, 164.1, 158.8, 147.2, 142.7, 135.7, 131.2, 130.7, 123.2, 119.2, 104.8, 62.8, 62.1, 55.6, 52.4, 50.7, 49.3, 43.8, 41.9, 34.9, 30.4, 28.8, 26.3, 24.9, 20.2, 19.5, 18.8; IR (KBr) ν_{max} 3329, 2937, 1743, 1672, 1638, 1495, 1462, 1416, 1255, 1136, 1019, 836 cm^{-1}; FABHRMS (NBA) *m/z* 1249.5890 (M + H$^+$, $C_{62}H_{80}N_{12}O_{16}$ requires 1249.5894).

*7.2.8 (N-(3-Benzyloxy-6-methylquinolinyl-2-carbonyl)-D-Ser-Pip-Gly-Sar-NMe-Val)$_2$ (serine hydroxyl) dilactone (**15**)*

0.012 mmol scale; flash chromatography (SiO_2, 1×16 cm, 0–5% EtOH–CH_2Cl_2 gradient) afforded **15** (14.5 mg, 17.2 mg theoretical, 84%) as white powder: R_f = 0.56 (40% CH_3CN–EtOAc); $[\alpha]_D^{23}$ −124 (*c* 0.24, $CHCl_3$); ^{1}H NMR ($CDCl_3$, 400 MHz) δ 9.03 (d, 2H, *J* = 6.3 Hz, Ser-NH), 8.48 (d, 2H, *J* = 4.5 Hz, Gly-NH), 7.81 (d, 2H, *J* = 8.6 Hz, C7-H), 7.55 (d, 2H, *J* = 7.4 Hz, C8-H), 7.50 (s, 2H, C4-H), 7.44 (s, 2H, C5-H), 7.41–7.35 (m, 8H), 7.32–7.26 (m, 2H, benzyl C4-H), 5.46 (d, 2H, *J* = 6.0 Hz, Pip-α-CH), 5.45 (d, 2H, *J* = 16.5 Hz, Sar-α-CH), 5.36–5.32 (m, 6H, Ser-α-CH and $PhCH_2$), 4.86 (dd, 2H, *J* = 11.6, 1.5 Hz, Ser-β-CH), 4.83 (d, 2H, *J* = 11.0 Hz, Val-α-CH), 4.58 (dd, 2H, *J* = 11.6, 2.6 Hz, Ser-β-CH), 4.42 (dd, 2H, *J* = 18.3, 5.6 Hz, Gly-α-CH), 4.10–3.98 (m, 4H, Gly-α-CH and Pip-ε-CH), 3.78–3.72 (m, 2H, Pip-ε-CH), 3.47 (d, 2H, *J* = 16.5 Hz, Sar-α-CH), 3.07 (s, 6H, Val-NCH_3), 2.92 (s, 6H, Sar-NCH_3), 2.50 (s, 6H, CH_3), 2.06 (d split septet, 2H, *J* = 11.0, 6.5 Hz, Val-β-CH), 1.80–1.45 (m, 12H, Pip$(CH_2)_3$), 0.95 (d, 6H, *J* = 6.5 Hz, Val-γ-CH_3), 0.81 (d, 6H, *J* = 6.5 Hz, Val-γ-CH_3); ^{13}C NMR ($CDCl_3$, 100 MHz) δ 172.7, 169.2, 169.1, 167.8, 167.1, 163.6, 151.9, 141.5, 140.3, 138.6, 136.1, 130.3, 129.9, 129.2, 128.7, 127.9, 126.9, 125.2, 116.7, 70.8, 62.9, 62.3, 52.5, 50.7, 49.3, 43.8, 41.9, 34.9, 30.4, 28.7, 26.5, 24.8, 21.8, 20.2, 19.4, 19.0; IR (KBr) ν_{max} 3328, 2928, 1743, 1675, 1639, 1491, 1415, 1352, 1261, 1190, 1136, 1017 cm^{-1}; FABHRMS (NBA-CsI) *m/z* 1561.5766 (M + H$^+$, $C_{76}H_{92}N_{12}O_{16}$ requires 1561.5809).

*7.2.9 (N-(3-Benzyloxy-7-chloroquinolinyl-2-carbonyl)-D-Ser-Pip-Gly-Sar-NMe-Val)$_2$ (serine hydroxyl) dilactone (**17**)*

0.0112 mmol scale; flash chromatography (SiO_2, 1×16 cm, 0–10% EtOH–CH_2Cl_2 gradient) afforded **17** (14.5 mg, 16.4 mg theoretical, 88%) as white powder: R_f = 0.32 (20% CH_3CN–EtOAc); $[\alpha]_D^{23}$ −138 (*c* 0.6, $CHCl_3$); ^{1}H NMR ($CDCl_3$, 400 MHz) δ 8.93 (d, 2H, *J* = 6.2 Hz, Ser-NH), 8.50 (d, 2H, *J* = 4.4 Hz, Gly-NH), 7.91 (d, 2H, *J* = 2.1 Hz, C8′-H), 7.63 (d, 2H, *J* = 8.8 Hz, C5-H), 7.57 (s, 2H, C4-H), 7.55 (m, 4H, phenyl C2′ and C6′-H), 7.47 (dd, 2H, *J* = 2.1, 8.8 Hz, C6-H), 7.42–7.37 (m, 4H, phenyl C3′ and C5′-H), 7.32–7.28 (m, 2H, phenyl C4′-H), 5.46 (d, 2H, *J* = 3.1 Hz, Pip-α-CH), 5.44 (d, 2H, *J* = 16.7 Hz, Sar-α-CH), 5.36–5.28 (m, 6H, D-Ser-α-CH and $PhCH_2$), 4.87 (dd, 2H, *J* = 2.8, 11.6 Hz, Ser-β-CH), 4.84 (d, 2H, *J* = 11.0 Hz, Val-α-CH) 4.58 (dd, 2H, *J* = 2.8, 11.6 Hz, Ser-β-CH), 4.43 (dd, 2H, *J* = 5.7, 18.3 Hz, Gly-α-CH), 4.03 (d, 2H, *J* = 18.3 Hz, Gly-α-CH), 4.01 (m, 2H, Pip-ε-CH), 3.75 (d, 2H, *J* = 13.5 Hz, Pip-ε-CH), 3.49 (d, 2H, *J* = 16.7 Hz, Sar-α-CH), 3.07 (s, 6H, Val-NCH_3), 2.93 (s, 6H, Sar-NCH_3), 2.08 (d split septet, 2H, *J* = 6.5, 11.0 Hz, Val-β-CH), 1.80–1.45 (m, 12H, Pip-$(CH_2)_3$), 0.95 (d, 6H, *J* = 6.5 Hz, Val-γ-CH_3), 0.82 (d, 6H, *J* = 6.5 Hz, Val-γ-CH_3); 13C NMR ($CDCl_3$, 100 MHz) δ 172.6, 169.3, 169.2, 167.8, 166.9, 163.1, 151.9, 143.6, 141.8, 135.8, 133.2, 129.4, 128.8, 128.6, 128.3, 128.0, 127.6, 126.9, 117.1, 70.9, 62.8, 62.2, 52.5, 50.8, 49.3, 43.9, 41.9, 34.9, 30.3, 28.7, 26.5, 24.8, 20.2, 19.4, 19.0; IR (KBr) ν_{max} 3323, 2938,1740, 1672, 1637, 1497, 1415, 1345, 1287, 1260, 1191, 1135, 1016, 940, 733 cm^{-1}; FABHRMS (NBA-CsI) *m/z* 1601.4828 (M + Cs$^+$, $C_{74}H_{86}Cl_2N_{12}O_{16}$ requires 1601.4716).

*7.2.10 (N-(Quinoxalyl-2-carbonyl)-D-Ser-Pip-Gly-Sar-NMe-Val)$_2$ (serine hydroxyl) dilactone (**18**)*

0.0091 mmol scale; flash chromatography (SiO_2, 1×16 cm, 5% EtOH–CH_2Cl_2 gradient) afforded **18** (9.3 mg, 10.8 mg theoretical, 86%) as white powder: R_f = 0.58 (10% EtOH–CH_2Cl_2); $[\alpha]_D^{23}$ −128 (*c* 0.44, $CHCl_3$); ^{1}H NMR ($CDCl_3$, 400 MHz) δ 9.66 (s, 2H, C3′-H), 8.54 (d, 2H, *J* = 4.7 Hz, Gly-NH), 8.18 (d, 2H, *J* = 8.2 Hz, C5′-H), 7.99 (d, 2H, *J* = 8.0 Hz, C8′-H), 7.90–7.79 (m, 4H, C6′ and C7′-H), 5.54 (d, 2H, *J* = 4.0 Hz, Pip-α-CH), 5.52 (d, 2H, *J* = 16.5 Hz, Sar-α-CH), 5.31 (d, 2H, *J* = 5.8 Hz, Ser-α-CH), 4.98 (d, 2H, *J* = 11.3 Hz, Ser-β-CH), 4.86 (d, 2H, *J* = 11.0 Hz, Val-α-CH), 4.49–4.40 (m, 4H, Ser-β-CH, and Gly-α-CH), 4.10–4.00 (m, 4H, Gly-α-CH and Pip-ε-CH), 3.76 (d, 2H, *J* = 13.3 Hz, Pip-

ε-CH), 3.53 (d, 2H, J = 16.5 Hz, Sar-α-CH), 3.09 (s, 6H, Val-NCH_3), 2.94 (s, 6H, Sar-NCH_3), 2.03 (d split septet, 2H, J = 6.5, 11.0 Hz, Val-β-CH), 1.82-1.50 (m, 12H, Pip-$(CH_2)_3$), 0.92 (d, 6H, J = 6.5 Hz, Val-γ-CH_3), 0.78 (d, 2H, J = 6.5 Hz, Val-γ-CH_3); ^{13}C NMR ($CDCl_3$, 100 MHz) δ 172.6, 169.4, 169.2, 167.7, 166.6, 162.6, 144.0, 143.8, 143.2, 140.4, 131.6, 130.7, 129.6, 129.5, 62.5, 62.0, 52.6, 50.8, 49.3, 43.9, 41.9, 34.9, 30.2, 28.7, 26.3, 24.9, 20.2, 19.4, 18.7; IR (KBr) ν_{max} 3330, 2938, 1745, 1682, 1638, 1509, 1491, 1417, 1283, 1136, 1015, 916, 776, 731 cm^{-1}; FABHRMS (NBA) m/z 1191.5591 ($M+H^+$, $C_{58}H_{74}N_{14}O_{14}$ requires 1191.5587).

*7.2.11 (N-(3-Benzyloxyquinoxalyl-2-carbonyl)-D-Ser-Pip-Gly-Sar-NMe-Val)$_2$ (serine hydroxyl) dilactone (**20**)*

0.0118 mmol scale; flash chromatography (SiO_2, 1×16 cm, 0–5% EtOH–CH_2Cl_2 gradient) afforded **20** (12.5 mg, 16.5 mg theoretical, 76%) as white powder: R_f = 0.22 (20% CH_3CN–EtOAc); $[\alpha]_D^{23}$ −128 (c 0.3, $CHCl_3$); ^1H NMR ($CDCl_3$, 400 MHz) δ 10.82 (d, 2H, J = 6.2 Hz, Ser-NH), 8.44 (d, 2H, J = 4.8 Hz, Gly-NH), 8.19 (dd, 2H, J = 1.3, 8.0 Hz, C8′-H), 7.57 (ddd, 2H, J = 1.3, 7.8, 8.0 Hz, C6′-H), 7.40 (dd, 2H, J = 7.4, 7.4 Hz, C7′-H), 7.33–7.18 (m, 12H, C5′-H and phenyl CH), 5.60–5.40 (m, 10H, Pip-α-CH, Sar-α-CH, Ser-α-CH, and $PhCH_2$), 4.87 (d, 2H, J = 11.1 Hz, Ser-β-CH), 4.82 (d, 2H, J = 11.0 Hz, Val-α-CH), 4.55 (dd, 2H, J = 2.8, 11.7 Hz, Ser-β-CH). 4.41 (dd, 2H, J = 5.8, 18.0 Hz, Gly-α-CH), 4.10-4.00 (m, 2H, Pip-ε-CH), 3.94 (d, 2H, J = 18.0 Hz, Gly-α-CH), 3.77–3.72 (m, 2H, Pip-ε-CH), 3.43 (d, 2H, J = 16.6 Hz, Sar-α-CH), 2.98 (s, 6H, Val-NCH_3), 2.89 (s, 6H, Sar-NCH_3), 2.05 (d split septet, 2H, J = 6.5, 11.0 Hz, Val-β-CH), 1.80–1.40 (m, 12H, Pip-$(CH_2)_3$), 0.94 (d, 6H, J = 6.5 Hz, Val-γ-CH_3), 0.79 (d, 6H, J = 6.5 Hz, Val-γ-CH_3); ^{13}C NMR ($CDCl_3$, 100 MHz) δ 172.6, 169.3, 169.0, 167.8, 166.3, 160.5, 155.0, 144.5, 134.7, 133.3, 133.2, 132.8, 132.6, 128.9, 127.8, 126.8, 124.6, 114.5, 62.8, 62.1, 52.4, 51.7, 49.3, 46.2, 43.9, 41.8, 34.9, 30.4, 28.9, 26.4, 24.9, 20.2, 19.4, 18.9; IR (KBr) ν_{max} 3321, 2396, 1741, 1684, 1638, 1497, 1464, 1283, 1136, 1017, 733 cm^{-1}; FABHRMS (NBA) m/z 1403.6430 ($M+H^+$, $C_{72}H_{86}N_{14}O_{16}$ requires 1403.6424).

*7.2.12 (N-(Isoquinolinyl-3-carbonyl)-D-Ser-Pip-Gly-Sar-NMe-Val)$_2$ (serine hydroxyl) dilactone (**21**)*

0.0148 mmol scale; flash chromatography (SiO_2, 2×15 cm, 5% EtOH–CH_2Cl_2 gradient) afforded **21** (16.5 mg, 17.6 mg theoretical, 94%) as white powder: R_f = 0.17 (10% CH_3CN–EtOAc); $[\alpha]_D^{23}$ −111 (c 0.24, $CHCl_3$); ^1H NMR ($CDCl_3$, 400 MHz) δ 9.42 (d, 2H, J = 6.3 Hz, Ser-NH), 9.11 (s, 2H, C4′-H), 8.59 (s, 2H, C1′-H), 8.51 (d, 2H, J = 4.6 Hz, Gly-NH), 7.99 (d, 2H, J = 8.0 Hz, C5′-H), 7.97 (d, 2H, J = 8.1 Hz, C8′-H), 7.74 (ddd, 2H, J = 1.2, 6.9, 8.1 Hz, C7′-H), 7.68 (ddd, 2H, J = 1.2, 6.9, 8.0 Hz, C6′-H), 5.50 (d, 2H, J = 5.2 Hz, Pip-α-CH), 5.49 (d, 2H, J = 16.5 Hz, Sar-α-CH), 5.31 (d, 2H, J = 6.3 Hz, Ser-α-CH), 4.90 (dd, 2H, J = 2.8, 11.7 Hz, Ser-β-CH), 4.84 (d, 2H, J = 11.0 Hz, Val-α-CH), 4.52 (dd, 2H, J = 2.8, 11.7 Hz, Ser-β-CH), 4.43 (dd, 2H, J = 5.9, 18.2 Hz, Gly-α-CH), 4.03 (m, 2H, Pip-ε-CH), 4.01 (d, 2H, J = 18.2 Hz, Gly-α-CH), 3.76 (d, 2H, J = 13.0 Hz, Pip-ε-CH), 3.49 (d, 2H, J = 16.5 Hz, Sar-α-CH), 3.06 (s, 6H, Val-NCH_3), 2.92 (s, 6H, Sar-NCH_3), 2.04 (d split septet, 2H, J = 6.5, 11.0 Hz, Val-β-CH), 1.80–1.45 (m, 12H, Pip-$(CH_2)_3$), 0.92 (d, 6H, J = 6.5 Hz, Val-γ-CH_3), 0.79 (d, 6H, J = 6.5 Hz, Val-γ-CH_3); ^{13}C NMR ($CDCl_3$, 100 MHz) δ 172.7, 169.3, 169.1, 167.8, 166.9, 164.3, 151.3, 143.4, 135.9, 130.9, 129.7, 128.8, 128.1, 127.5, 120.3, 62.9, 62.1, 52.4, 50.7, 49.3, 43.8, 41.8, 34.9, 30.4, 28.7, 26.4, 24.8, 20.2, 19.4, 18.8; IR (KBr) ν_{max} 3497, 3328, 2938, 1742, 1639, 1505, 1436, 1287, 1 136, 1095, 1016, 920 cm^{-1}; FABHRMS (NBA-CsI) m/z 1321.4670 ($M+Cs^+$, $C_{60}H_{76}N_{12}O_{14}$ requires 1321.4658).

*7.2.13 (N-(Isoquinolinyl-1-carbonyl)-D-Ser-Pip-Gly-Sar-NMe-Val)$_2$ (serine hydroxyl) dilactone (**22**)*

0.0139 mmol scale; flash chromatography (SiO_2, 2×15 cm, 0–5% EtOH–CH_2Cl_2 gradient) afforded **22** (13.6 mg, 16.5 mg theoretical, 82%) as white powder: R_f = 0.31 (10% CH_3CN–EtOAc); $[\alpha]_D^{23}$ −74 (c 1.15, $CHCl_3$); ^1H NMR ($CDCl_3$, 400 MHz) δ 9.56 (d, 2H, J = 1.6, 8.2 Hz, C8′-H), 9.39 (d, 2H, J = 6.3 Hz, Ser-NH), 8.51 (d, 2H, J = 4.8 Hz, Gly-NH), 8.42 (d, 2H, J = 5.4 Hz, C3′-H), 7.83 (dd, 2H, J = 2.0, 7.1 Hz, C5′-H), 7.77 (d, 2H, J = 5.4 Hz, C4′-H), 7.72–7.65 (m, 4H, C6′ and C7′-H), 5.49 (d, 2H, J = 5.0 Hz, Pip-α-CH), 5.47 (d, 2H, J = 16.6 Hz, Sar-α-CH), 5.31 (d, 2H, J = 6.3 Hz, Ser-α-CH), 4.90 (dd, 2H, J = 1.6, 11.7 Hz, Ser-β-CH), 4.85 (d, 2H, J = 11.0 Hz, Val-α-CH), 4.54 (dd, 2H, J = 2.8, 11.7 Hz, Ser-β-CH), 4.43 (dd, 2H, J = 5.9, 18.3 Hz, Gly-α-CH), 4.04 (m, 2H, Pip-ε-CH), 4.00 (d, 2H, J = 18.3 Hz, Gly-α-CH), 3.77 (d, 2H, J = 13.3 Hz, Pip-ε-CH), 3.48 (d, 2H, J = 16.6 Hz, Sar-α-CH), 3.05 (s, 6H, Val-NCH_3), 2.92 (s, 6H, Sar-NCH_3), 2.07 (d split septet, 2H, J = 6.6, 11.0 Hz, Val-β-CH), 1.80–1.45 (m, 12H, Pip-$(CH_2)_3$), 0.94 (d, 6H, J = 6.6 Hz, Val-γ-CH_3), 0.80 (d, 6H, J = 6.6 Hz, Val-γ-CH_3); ^{13}C NMR ($CDCl_3$, 100 MHz) δ 172.7, 169.4, 169.1, 167.8, 167.0, 165.5, 147.6, 140.5, 137.3, 130.4, 128.6, 127.6, 127.1, 126.8, 124.3, 62.8, 62.1, 52.5, 50.7, 49.3, 43.8, 41.8, 34.9, 30.4, 28.7, 26.4, 24.9, 20.1,19.5,18.9; IR (KBr) ν_{max} 3518, 3325, 2936, 1744, 1668, 1638, 1505, 1490, 1463, 1417, 1287, 1259, 1136, 1017, 837 cm^{-1}; FABHRMS (NBA-CsI) m/z 1321.4739 ($M+Cs^+$, $C_{60}H_{76}N_{12}O_{14}$ requires 1321.4658).

*7.2.14 (N-(3-Hydroxynaphthyl-2-carbonyl)-D-Ser-Pip-Gly-Sar-NMe-Val)$_2$ (serine hydroxyl) dilactone (**5**)*

0.0112 mmol scale; flash chromatography (SiO_2, 2×15 cm, 40% CH_3CN–EtOAc) afforded **5** (11.0 mg,

13.7 mg theoretical, 80%) as a white powder: $R_f = 0.56$ (40% CH_3CN–EtOAc); $[\alpha]_D^{23}$ −102 (*c* 0.26, $CHCl_3$); ^1H NMR ($CDCl_3$, 400 MHz) δ 11.60 (s, 2H, OH), 8.58 (d, 2H, $J = 4.3$ Hz, Ser-NH), 8.17 (d, 2H, $J = 5.2$ Hz, Gly-NH), 7.96 (s, 2H, C4-H), 7.71 (d, 2H, $J = 8.4$ Hz, C5-H), 7.68 (d, 2H, $J = 8.5$ Hz, C8-H), 7.47 (dd, 2H, $J = 7.5$, 7.7 Hz, C7-H), 7.31 (s, 2H, Cl-H), 7.30 (dd, 2H, $J = 7.5$, 7.7 Hz, C6-H), 5.42 (d, 2H, $J = 5.8$ Hz, Pip-α-CH), 5.40 (d, 2H, $J = 16.5$ Hz, Sar-α-CH), 5.26 (br s, 2H, Ser-α-CH), 4.84 (d, 2H, $J = 11.0$ Hz, Val-α-CH), 4.80 (d, 2H, $J = 11.8$ Hz, Ser-β-CH), 4.64 (dd, 2H, $J = 11.8$, 1.2 Hz, Ser-β-CH), 4.46 (dd, 2H, $J = 18.4$, 5.2 Hz, Gly-α-CH), 4.07 (d, 2H, $J = 18.4$ Hz, Gly-α-CH), 4.01 (m, 2H, Pip-ε-CH), 3.75 (m, 2H, Pip-ε-CH), 3.49 (d, 2H, $J = 16.5$ Hz, Sar-α-CH), 3.01 (s, 6H, Val-NCH_3), 2.96 (s, 6H, Sar-NCH_3), 2.07 (d split septet, 2H, $J = 11.0$, 6.5 Hz, Val-β-CH), 1.80–1.45 (m, 12H, Pip$(CH_2)_3$), 0.95 (d, 6H, $J = 6.5$ Hz, Val-γ-CH_3), 0.82 (d, 6H, $J = 6.5$ Hz, Val-γ-CH_3); ^{13}C NMR ($CDCl_3$, 100 MHz) δ 172.4, 169.4, 169.2, 168.9, 167.6, 166.8, 156.8, 137.1, 128.6, 128.5, 127.2, 126.8, 126.3, 123.9, 116.6, 112.4, 62.6, 62.2, 52.8, 51.0, 49.3, 44.0, 41.9, 35.1, 30.1, 28.4, 26.6, 24.7, 20.0, 19.3, 18.9; IR (KBr) ν_{max} 3321, 2938, 1743, 1667, 1638, 1509, 1463, 1417, 1287, 1232, 1135, 1016, 919, 730 cm^{-1}; FABHRMS (NBA) *m/z* 1219.5640 ($M + H^+$, $C_{62}H_{78}N_{10}O_{16}$ requires 1219.5676).

7.2.15 N-*(3-Hydroxypyridyl-2-carbonyl)*-D-*Ser-Pip-Gly-Sar-NMe-Val)$_2$ (serine hydroxyl) dilactone (**8**)*

0.0062 mmol scale; flash chromatography (SiO_2, 1×16 cm, 0–5% EtOH–CH_2Cl_2 gradient) afforded **8** (6.6 mg, 7.0 mg theoretical, 94%) as a white powder: $R_f = 0.62$ (10% EtOH–CH_2Cl_2); $[\alpha]_D^{23}$ −85 (*c* 0.21, $CHCl_3$); ^1H NMR ($CDCl_3$, 400 MHz) δ 11.87 (s, 2H, OH), 9.22 (d, 2H, $J = 6.2$ Hz, Ser-NH), 8.50 (d, 2H, $J = 5.1$ Hz, Gly-NH), 8.01 (dd, 2H, $J = 3.9$, 1.7 Hz, C4-H), 7.33–7.26 (m, 4H, C5-H and C6-H), 5.48 (d, 2H, $J = 5.8$ Hz, Pip-α-CH), 5.46 (d, 2H, $J = 16.5$ Hz, Sar-α-CH), 5.19 (d, 2H, $J = 6.2$ Hz, Ser-α-CH), 4.85 (d, 4H, $J = 11.0$ Hz, Val-α-CH and Ser-β-CH), 4.47 (dd, 2H, $J = 12.1$, 2.7 Hz, Ser-β-CH), 4.42 (dd, 2H, $J = 18.5$, 5.8 Hz, Gly-α-CH), 4.06–3.98 (m, 4H, Gly-α-CH and Pip-ε-CH), 3.70 (d, 2H, $J = 13.1$ Hz, Pip-ε-CH), 3.48 (d, 2H, $J = 16.5$ Hz, Sar-α-CH), 3.01 (s, 6H, Val-NCH_3), 2.92 (s, 6H, Sar-NCH_3), 2.07 (d split septet, 2H, $J = 11.0$, 6.5 Hz, Val-β-CH), 1.80–1.50 (m, 12H, Pip-$(CH_2)_3$), 0.95 (d, 6H, $J = 6.5$ Hz, Val-γ-CH_3), 0.81 (d, 6H, $J = 6.5$ Hz, Val-γ-CH_3); ^{13}C NMR ($CDCl_3$, 100 MHz) δ 172.6, 169.4, 169.1, 168.3, 167.7, 166.3, 157.8, 139.8, 131.3, 128.6, 125.9, 62.5, 52.5, 50.3, 49.3, 43.9, 41.8, 34.9, 30.3, 28.7, 26.4, 24.8, 20.1, 19.4,18.8; IR (KBr) ν_{max} 3327, 2930, 1744, 1672, 1638, 1519, 1450, 1294, 1135, 1016, 919 cm^{-1}; FABHRMS (NBA) *m/z* 1121.5198 ($M + H^+$, $C_{52}H_{72}N_{12}O_{16}$ requires 1121.5268).

*7.2.16 (*N-*(3-Hydroxy-6-methylquinolinyl-2-carbonyl)*-D-*Ser-Pip-Gly-Sar-NMe-Val)$_2$ (serine hydroxyl) dilactone (**14**)*

0.0063 mmol scale; flash chromatography (SiO_2, 1×16 cm, EtOAc) afforded **14** (7.2 mg, 7.9 mg theoretical, 91%) as a white powder: $R_f = 0.56$ (EtOAc); $[\alpha]_D^{23}$ −153 (*c* 0.24, $CHCl_3$); ^1H NMR ($CDCl_3$ 400 MHz) δ 11.71 (s, 2H, OH), 9.51 (d, 2H, $J = 5.9$ Hz, Ser-NH), 8.52 (d, 2H, $J = 3.8$ Hz, Gly-NH), 7.69 (d, 2H, $J = 8.7$ Hz, C7-H), 7.52 (s, 2H, C4-H), 7.45 (s, 2H, C5-H), 7.32 (d, 2H, $J = 8.3$ Hz, C8-H), 5.56 (d, 2H, $J = 5.3$ Hz, Pip-α-CH), 5.54 (d, 2H, $J = 16.5$ Hz, Sar-α-CH), 5.25 (d, 2H, $J = 5.9$ Hz, Ser-α-CH), 4.97 (d, 2H, $J = 11.6$ Hz, Ser-β-CH), 4.86 (d, 2H, $J = 11.0$ Hz, Val-α-CH), 4.43 (m, 4H, Ser-β-CH and Gly-α-CH), 4.05 (m, 4H, Gly-α-CH and Pip-ε-CH), 3.73 (m, 2H, Pip-ε-CH), 3.55 (d, 2H, $J = 16.5$ Hz, Sar-α-CH), 3.11 (s, 6H, Val-NCH_3), 2.94 (s, 6H, Sar-NCH_3), 2.50 (s, 6H, CH_3), 2.03 (d split septet, 2H, $J = 11.0$, 6.5 Hz, Val-β-CH), 1.85–1.50 (m, 12H, Pip$(CH_2)_3$), 0.92 (d, 6H, $J = 6.5$ Hz, Val-γ-CH_3), 0.78 (d, 6H, $J = 6.5$ Hz, Val-γ-CH_3); ^{13}C NMR ($CDCl_3$, 100 MHz) δ 172.6, 169.4, 169.2, 167.9, 167.7, 166.3, 153.9, 140.2, 138.8, 133.8, 132.2, 129.7, 129.1, 125.1, 119.5, 62.3, 62.0, 52.5, 50.5, 49.3, 43.9, 41.9, 34.9, 30.3, 28.8, 26.2, 24.9, 21.8, 20.2, 19.4, 18.7; IR (KBr) ν_{max} 3330, 2934, 1746, 1672, 1640, 1519, 1469, 1416, 1338, 1286, 1191, 1135, 1096, 1016, 909, 820, 734 cm^{-1}; FABMS (NBA) *m/z* 1250 ($M + H^+$).

*7.2.17 (*N-*(7-Chloro-3-hydroxyquinolinyl-2-carbonyl)*-D-*Ser-Pip-Gly-Sar-NMe-Val)$_2$ (serine hydroxyl) dilactone (**16**)*

0.0094 mmol scale; flash chromatography (SiO_2, 1×16 cm, EtOAc) afforded **16** (9.4 mg, 12.1 mg theoretical, 78%) as white powder: $R_f = 0.52$ (20% CH_3CN–EtOAc); $[\alpha]_D^{23}$ −168 (*c* 0.6, $CHCl_3$); ^1H NMR ($CDCl_3$, 400 MHz) δ 11.82 (s, 2H, OH), 9.51 (br s, 2H, Ser-NH), 8.55 (br s, 2H, Gly-NH), 7.82 (s, 2H, C4-H), 7.66–7.61 (m, 4H, C6 and C8-H), 7.45 (d, 2H, $J = 8.6$ Hz, C5-H), 5.57 (d, 2H, $J = 4.8$ Hz, Pip-α-CH), 5.53 (d, 2H, $J = 16.5$ Hz, Sar-α-CH), 5.24 (br s, 2H, Ser-α-CH), 4.98 (d, 2H, $J = 11.4$ Hz, Ser-β-CH), 4.87 (d, 2H, $J = 11.0$ Hz, Val-α-CH), 4.44 (m, 4H, Ser-β-CH and Gly-α-CH), 4.05 (m, 4H, Gly-α-CH and Pip-ε-CH), 3.74 (m, 2H, Pip-ε-CH), 3.57 (d, 2H, $J = 16.5$ Hz, Sar-α-CH), 3.10 (s, 6H, Val-NCH_3), 2.95 (s, 6H, Sar-NCH_3), 2.05 (d split septet, 2H, $J = 11.0$, 6.5 Hz, Val-β-CH), 1.80–1.50 (m, 12H, Pip-$(CH_2)_3$), 0.92 (d, 6H, $J = 6.5$ Hz, Val-γ-CH_3), 0.79 (d, 6H, $J = 6.5$ Hz, Val-γ-CH_3); ^{13}C NMR ($CDCl_3$, 100 MHz) δ 172.6, 169.4, 169.1, 167.8, 167.4, 166.1, 154.1, 141.5, 135.4, 132.8, 130.3, 129.6, 128.0, 127.6, 120.5, 62.2, 61.9, 52.6, 50.7, 49.3, 43.9, 41.9, 34.9, 30.2, 28.8, 26.3, 24.9, 20.2, 19.4, 18.7; IR (KBr) ν_{max}, 3328, 2939, 1745, 1667, 1641, 1519, 1417, 1333, 1287, 1191, 1136, 1094, 1017, 917, 731 cm^{-1}; FABHRMS (NBA-CsI) *m/z* 1421.3715 ($M + Cs^+$, $C_{60}H_{74}Cl_2N_{12}O_{16}$ requires 1421.3777).

7.3 DNA binding studies. Analog solution preparation

The analogs were dissolved in DMSO to a concentration of 1×10^{-3} M. These solutions were stored under Ar at −78°C and the integrity of the agents was checked periodically by ^{1}H NMR in 10% DMSO-d_6/$CDCl_3$. In most cases, a final cuvette concentration of 1×10^{-5} M in a 2 ml aqueous buffer containing 10 mM NaCl, 75 mM Tris-HCl (pH 7.4) was achieved by adding 20 μl of the analog solution to the buffer. An additional 20 μl DMSO was added to promote dissolution of the analogs in the aqueous buffer.

7.4 Calf thymus DNA

Type I calf thymus DNA (Sigma) was dissolved in aqueous buffer containing 10 mM NaCl, 75 mM Tris-HCl (pH 7.4). The concentration in base-pairs, was obtained by UV spectroscopy at 24°C based on a base-pair extinction coefficient of 12824 M^{-1} cm^{-1} at 260 nm [27]. The purity was checked by assuring that the absorbance ratio at 260:280 nm was greater than 1.8 [28].

7.5 Deoxyoligonucleotides

The following self-complementary deoxyoligonucleotides: 5′-$(GCATGC)_2$, 5′-$d(GCTAGC)_2$, 5′-$d(GCGCGC)_2$, 5′-$d(GCCGGC)_2$, and 5′-$d(CGTACG)_2$, were prepared on-site (The Scripps Research Institute Core Facility) or by Biosource Intl (Camarillo, CA) and were purified by isopropanol precipitation. Quantitation of the DNA concentration was established by UV absorbance (260 nm) of the single-strand DNA (75°C) and the concentrations were established using the calculated extinction coefficients of 55200, 55800, 51000, 51600, and 57600 M^{-1} cm^{-1}, respectively [29]. The results for 5′-$d(GCATGC)_2$ were compared with concentrations established by ^{1}H NMR where the thymine methyl signal was integrated against an internal standard of deuterated trimethylsilyl sodium propionate. Concentrations obtained by both methods were in agreement.

7.6 DNA binding constant measurements by fluorescence quenching

A 20 μl aliquot of a 1 mM DMSO solution of the agent was added to 1960 μl of aqueous buffer (10 mM Tris-HCl, pH 7.4, 75 mM NaCl) in a 4 ml quartz cuvette equipped with a Teflon coated stir bar to achieve a final concentration of 10 μM. An additional 20 μl of DMSO was added to the cuvette to increase solubility of the agent and the solutions were shielded from light. After 5 min of stirring, an initial fluorescence reading was taken with minimum exposure to the excitation beam. At this point, aliquots of the DNA solution (5–30 μl depending on amount necessary to maximize titration points in the high affinity binding region of the Scatchard plot) were added and the solution was allowed to equilibrate 15 min before the subsequent readings were taken. The excitation and emission wavelengths used for each analog varied and can be found in Table 1. The results of the titration were analyzed by Scatchard analysis [18]. The linear portion of the Scatchard plot was used to determine the high affinity binding constants. In the case of the deoxyoligonucleotide study, a non-linear fit of the curve as described in the text was also used to determine the high affinity binding constant [21].

7.7 Inhibition of HIV-1 reverse transcriptase

The assay was performed according to an available procedure [26] with slight modification. A 45 μl solution of reaction buffer containing 55 mM Tris·HCl, pH 8.2, 80 mM potassium chloride, 12 mM $mgCl_2$, 1 mM DTT, 50 μM EGTA, 2.5 μg/ml rA·dT, 0.5 μCi of [^{3}H]TTP, 10 μM TTP, 1 mg/ml BSA, and 0.01% Triton X-100 was added to a well in a filter cluster plate (Millipore MAHV N45). The reverse transcription reaction was initiated upon addition of the reverse transcriptase (1 unit; 1 unit = 10 pmol of [^{3}H]TMP incorporated/60 min at 37°C). The plate was incubated at 37°C for 90 min. The plate was then placed on ice and 200 μl of 13% trichloroacetic acid and 10 mM sodium pyrophosphate was added to each well. The plate was chilled for 2 h and the liquid vacuumed out through the filter using a Millipore manifold (Millipore MAVM 09601). The precipitate was washed with 1 M and 10 mM sodium pyrophosphate twice. The filter was punched out and placed in a scintillation vial. A 4 ml of cocktail was added. Radioactivity was determined by liquid scintillation counting.

The effects of sandramycin and its analogs on HIV-1 reverse transcriptase were determined by incubating the agents and the rA·dT containing buffer at 25°C for 30 min prior to addition of the reverse transcriptase. Reactions containing no agents were used as controls, and those lacking the transcriptase were used as blanks.

Acknowledgements

We gratefully acknowledge the financial support of the National Institutes of Health (CA 41101) and The Skaggs Institute for Chemical Biology.

References

[1] Matson JA, Bush JA. J Antibiot 1989;42:1763.
[2] Matson JA, Colson KL, Belofsky GN, Bleiberg BB. J Antibiot 1993;46:162.

[3] (a) Ohkuma H, Sakai F, Nishiyama Y, Ohbayashi M, Imanishi H, Konishi M, Miyaki T, Koshiyama H, Kawaguchi H. J Antibiot 1980;33:1087. Tomita K, Hoshino Y, Sasahira T, Kawaguchi H. J Antibiot 1980;33:1098. Konishi M, Ohkuma H, Sakai F, Tsuno T, Koshiyama H, Naito T, Kawaguchi H. J Antibiot 1981;34:148. (b) Konishi M, Ohkuma H, Sakai F, Tsuno T, Koshiyama H, Naito T, Kawaguchi H. J Am Chem Soc 1981;103:1241. (c) Arnold E, Clardy J. J Am Chem Soc 1981;103:1243.
[4] Toda S, Sugawara K, Nishiyama Y, Ohbayashi M, Ohkusa N, Yamamoto H, Konishi M, Oki T. J Antibiot 1990;43:796.
[5] Lingham RB, Hsu AHM, O'Brien JA, Sigmund JM, Sanchez M, Gagliardi MM, Heimbuch BK, Genilloud O, Martin I, Diez MT, Hirsch CF, Zink DL, Liesch JM, Koch GE, Gartner SE, Garrity GM, Tsou NN, Salituro GM. J Antibiot 1996;49:253.
[6] Boger DL, Chen J-H, Saionz KW. J Am Chem Soc 1996;118:1629. Boger DL, Chen J-H. J Am Chem Soc 1993;115:11624. For a preliminary disclosure of **4**: see Boger DL, Chen J-H. Bioorg Med Chem Lett 1997;7:919.
[7] Fox KR, Woolley C. Biochem Pharmacol 1990;39:941. Fox KR, Davies H, Adams GR, Portugal J, Waring M. J Nucl Acids Res 1988;16:2489.
[8] Huang C-H, Mong S, Crooke ST. Biochemistry 1980;19:5537. Huang C-H, Prestayko AW, Crooke ST. Biochemistry 1982;21:3704. Huang C-H, Crooke ST. Cancer Res 1985;45:3768. Huang C-H, Mirabelli CK, Mong S, Crooke ST. Cancer Res 1983;43:2718.
[9] Leroy JL, Gao X, Misra V, Gueron M, Patel D. J. Biochemistry 1992;31:1407. Zhang X, Patel D. J Biochemistry 1991;30:4026. Searle MS, Hall JG, Denny WA, Wakelin LPG. Biochem J 1989;259:433. Searle MS, Hall JG, Wakelin LPG. Biochem J 1988;256:271. Searle MS, Hall JG, Penny WA, Wakelin LPG. Biochemistry 1988;27:4340.
[10] Waring MJ, Fox KR. In: Neidle S, Waring MJ, editors. Mol. Aspects Anti-cancer Drug Action. Weinheim: Verlag, 1983:127. Waring MJ. In: Neidle S, Waring MJ, editors. Mol. Aspects Anti-cancer Drug-DNA Interact. Basingstoke:MacMillan, 1993:213. UK-63052 and related agents: Rance MJ, Ruddock JC, Pacey MS, Cullen WP, Huang LH, Jefferson MT, Whipple EB, Maeda H, Tone J. J Antibiot 1989;42:206. Fox KR. J Antibiot 1990;43:1307.
[11] Wang AH-J, Ughetto G, Quigley GJ, Hakoshima T, van der Marel GA, van Boom JH, Rich A. Science 1984;225:1115. Ughetto G, Wang AH-J, Quigley GJ, van der Marel GA, van Boom JH, Rich A. Nucl Acids Res 1985;13:2305. Van Dyke MM, Dervan PB. Science 1984;225:1122. Low CML, Olsen RK, Waring MJ. FEBS Letters 1984;176:414.
[12] Chen H, Patel DJ. J Mol Biol 1995;246:164. Bailly C, Hamy F, Waring M. J Biochemistry 1996;35:1150. Fletcher MC, Fox KR. Biochemistry 1996;35:1064.
[13] Take Y, Inouye Y, Nakamura S, Allaudeen HS, Kubo A. J Antibiot 1989;42:107. Inouye Y, Take Y, Nakamura S, Nakashima H, Yamamoto N, Kawaguchi H. J Antibiot 1987;40:100.
[14] Cheng C-C, Yan S-J. Org React 1982;28:37.
[15] Boger DL, Chen J-H. J Org Chem 1995;60:7369.
[16] Boger DL, Brotherton CE, Panek JS, Yohannes D. J Org Chem 1984;49:4056.
[17] Birdsall B, King RW, Wheeler MR, Lewis CA Jr, Goode SR, Dunlap RB, Roberts GCK. Analytical Biochem 1983;132:353.
[18] Scatchard G. Ann N Y Acad Sci 1949;51:660.
[19] Chaires JB. In: Hurley LH, editor. Advances in DNA Sequence Specific Agents. Greenwich:JAI, 1992;1:3–23. Deranleau DA. J Am Chem Soc 1969;91:4050. Kermode JC. Biochem Pharmacol 1989;38:2053.
[20] Nørby JG, Ottolenghi P, Jensen J. Anal Biochem 1980;102:318. Zieler K. Trends Biochem Sci 1989;14:314.
[21] Feldman HA. Anal Biochem 1972;48:317.
[22] SAS Institute Inc., SAS Campus Drive, Cary, NC 27513.
[23] Attempts to confirm bis-intercalation of sandramycin about the central 5′-GC base-pairs of 5′-d$(GCGCGC)_2$ by ^{1}H NMR of a symmetrical 1:1 complex were not successful and suggested multiple binding sites within this deoxyoligonucleotide.
[24] Johnson DS, Boger DL. In: Lehn J-M, editor. Comprehensive Supramolecular Chemistry. Oxford:Pergamon, 1996;4:73–176.
[25] Tan GT, Miller JF, Kingshorn DA, Hughes SH, Pezzuto JM. Biochem Biophys Res Commun 1992;185:370.
[26] Goldman ME, Salituro GS, Bowen JA, Williamson JM, Zink DL, Schleif WA, Emini EA. Mol Pharmacol 1990; 38:20.
[27] Dienes Z, Vogel P. Bioorg Med Chem Lett 1995;5:547.
[28] Maniatis T, Fritsch EF, Sambrook J. Mol. Cloning: A Laboratory Manual. New York:Cold Spring Harbor, 1982:468–469.
[29] Richards EG. In: Fasman GD, editor. Handbook of Bochemisry and Molecular Biology: Nucleic Acids, Cleveland:CRC, 3rd ed., 1975;1:597. Borer PN. In: Fasman GD, editor. Handbook of Biochemisty and Molecular Biology: Nucleic Acids, Cleveland:CRC, 3rd ed., 1975;1:589.